Journal of Power Sources 451 (2020) 227794

Contents lists available at ScienceDirect

Journal of Power Sources

journal homepage: www.elsevier.com/locate/jpowsour

Review article

Recent progress of biomass-derived carbon materials for supercapacitors

Jiashuai Wang [a], Xiao Zhang [a], Zhe Li [a], Yanqing Ma [a,b,*], Lei Ma [a,**]

[a] Tianjin International Center for Nanoparticles and Nanosystems, Tianjin University, 300072, PR China
[b] State Laboratory of Precision Measuring Technology and Instruments, Tianjin University, 300072, PR China

HIGHLIGHTS

- Synthesis of carbon materials from different biomass precursors.
- Relationship between biochar structure and capacitive performance.
- Prediction the electrochemical properties by machine learning method.
- Current challenges and new trends on the biomass-based materials in supercapacitors.

GRAPHICAL ABSTRACT

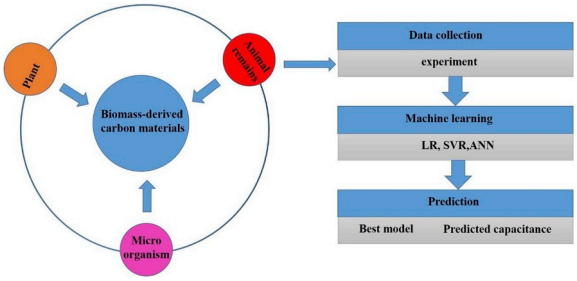

ARTICLE INFO

Keywords:
Biomass
Supercapacitors
Structure-performance relationship
Theoretical prediction

ABSTRACT

The carbon material based biomass in energy storage has attracted much interest due to their environmental friendly, natural abundance and special porous structures. In this paper, the relationship between the species of biomass-based electrode and properties of supercapacitors are systematically discussed. On the one hand, the influence of the specific morphologies, heteroatom-introducing and graphitization degree of active carbon on the electrochemical properties are analyzed in detail, which give a promising direction for biomass-based carbon in clean energy field. On the other hand, machine learning, especially artificial neural network model, has been widely used as data mining technology to predict the electrochemical properties of electrode materials. It makes the structure-performance relationship for biomass-based supercapacitors more specifically. Current development in synthesis of active carbon from biomass combined with theoretical prediction is summarized, which provides a meaningful guidance into the application of energy storage supercapacitors. Current challenges and new trends on the biomass-based carbon materials in supercapacitors have also been proposed.

1. Introduction

With the exhausting energy and polluting environment, energy is becoming an important factor to restrict development of economy [1]. However, recent energy consumption is mostly dependent on irreplaceable fossil fuels [2]. In order to provide a green energy source, some researchers are devoted to develop clean and renewable energy like wind, solar, and tide [3]. The problem that power acquisition is mainly intermittent need to be settled [4]. In addition to the increasing of portable and miniaturized electronic equipment, means efficient electrical energy storage materials and technology should be come out [5]. To date, among various devices for energy storage, lithium-ion

* Corresponding author. Tianjin International Center for Nanoparticles and Nanosystems, Tianjin University, 300072, PR China.
** Corresponding author.
E-mail addresses: mayanqing@tju.edu.cn (Y. Ma), lei.ma@tju.edu.cn (L. Ma).

https://doi.org/10.1016/j.jpowsour.2020.227794
Received 15 October 2019; Received in revised form 21 January 2020; Accepted 22 January 2020
Available online 12 February 2020

batteries (LIBs) are aroused attention on account of their high gravimetric energy density. Yet, LIBs still suffer from low power density and slow energy delivery [6]. Consequently, other applicable devices in energy storage market should be evolved. For this matter, supercapacitors (SCs) have attained much interest on account of their quick charge/discharge rate, long cycle life, and more adaptable to severe condition than that of LIBs [7]. Importantly, with the growing development of the electric vehicles, endowed supercapcitors become to be the potential electrochemical capacitors. In principle, SCs can provide high power density and rate response in need [8]. However, the low energy density is one weakness limits widespread in SCs [9,10]. Hence, scientific researchers make efforts to improve the energy density ability through developing new energy storage materials, optimizing electrolytes with a high operation potential [11].

Briefly, supercapacitors are generally classified into two types based on their storage mechanism: the electrochemical double layer capacitors (EDLCs) and pseudocapacitors. EDLCs store charges via reversible ion adsorption at the electrode–electrolyte interface, while pseudocapacitors store charges via redox reaction [6]. The electrode materials for the former are mainly carbon-based materials including activated carbon, carbon nanotubes, and graphene. While for the latter they can be metal oxides and conducting polymers. Generally, pseudocapacitive materials exhibit a higher specific capacitance than EDLCs electrodes. However, carbon-based materials tend to have a better cycle stability and rate capability. Therefore, porous materials have been the focus on searching for advanced electrode materials for SCs [13,14]. Reasonable designs of electrode materials, including the specific surface area, surface morphology and graphitization degree, are significant factors to achieve excellent performance [6]. In the range of the employed energy storage materials, carbon-based materials have aroused much attention on account of their high specific surface area, hierarchical porous frameworks and good structural stability [7]. So SCs can achieve high specific capacitance, high charge/discharge rates and a long lifetime. Researchers have successfully synthesized nanostructured carbon materials from 0D to 3D for electrodes of SCs [8,9]. Graphene or carbon nanotube, being popular carbon materials, shows superior framework as well as competitive chemical performance [10,11]. Although such successful application, there are still a lot of problems related to energy storage materials. For instance, graphene is usually synthesized from fossil fuel by chemical vapor deposition method, which is faced challenge of environmental degradation and unsustainability [20]. Graphite and petroleum coke-derived active carbon are nonrenewable and contaminative. Moreover, nanostructured carbons from them are often obtained under very harsh conditions [12]. Biomass including renewable crops or animals can be regarded as an environment-friendly precursor which brings less pollution to the atmosphere. Biomass with naturally hierarchical structures as precursor could be a realistic alternative among energy storage materials. Giving biomass is derived from renewable crops or animal, so that show cheaper than other kinds of nanostructure materials. There has also been a lot of research currently regarding with preparation of electrode from extensively renewable biomass. On the one hand, biomass is the most available carbon precursor from plant, animal or marine organism. These resources on earth are abundant and cheap. On the basis of a survey, the yield of crops reaches around 146 billion tons every year [13]. On the other hand, the living waste or animal husbandry is produced about 100 billion tons according to statistics [14]. This can result in a waste and an urgent environmental issue. So the usage of biomass in the production of activated carbon for supercapacitors electrodes is considered as an effective way of settling disposal problem from the agricultural or living wastes [15]. Biomass-based active electrode materials can inherit or form particular porous and layered structures by simple method [25]. These days, the use of biomass to formation activated electrode materials for electrochemical energy storage field has attract much interest [16,17]. Lots of biomass-based active electrode materials have been prepared through hydrothermal carbonization, chemical or physical activation. For example, Jiang et al. provided a summary of recent progress on the well-design of biomass-derived carbon materials, focusing on morphologies, surface chemistry and synthesis method for their applications in supercapacitors, lithium- and sodium-ion batteries [18]. Bi et al. reviewed recent developments of biomass-derived porous carbon materials with different dimensions and their applications as carbon-based electrode materials for supercapacitors [19]. Yang et al. summarized the application of hierarchical porous carbons derived from biomass including lignin, alginate, starch, chitin, gelatin, emphasizing on the relationship between the pore structure and electrochemical efficiency [20]. Lu et al. mainly discussed cellulose-, lignin- and hemicellulose-derived carbon electrode materials for supercapacitor applications [21]. However, there is no review on the structure and composition of biomass from precursor perspective. Natural biomass with an interconnected channels and a diverse of microstructures are necessary to product porous materials, so affect the specific surface area of carbonized materials. Thus, it was thought useful to critically discuss the potential precursor selection from diverse biomass. This review is to highlight the recent advances in the synthesis of carbon materials from different biomass precursors. The effects of the pore structure, surface properties, and graphitic degree on the electrochemical performance are discussed in detail, which will guide further rational design of the biomass-derived carbon materials for supercapacitors. In addition, we provide a summary about combination of data science and experiments to establish high-level connections between structure features and the electrochemical properties, which unravel the most significant factors on the capacitance and power density of supercapacitors. Finally, the current challenge and new outlook in biomass-based active electrode materials development have also been discussed.

2. Precursors in biomass-derived materials

Biomass obtained from terrestrial plant, marine organism, and daily waste may be applied to prepare active carbon in electrode materials. In recent years, biomass-based materials or byproducts have been utilized as a sustainable precursors to prepare carbon nanomaterials for energy storage, including algae, [22], catkins [23], rice [24], orange peel [25], sugar cane bagasse [26], camellia pollen [27], rice stem [28], coconut shell [29], sunflower stalk [30], tamarind seed coat [31], almonds [32], Jujun grass [33], etc. Their intrinsic microstructural characteristic and chemical composition vary from one species to another. Biomass can be used as a precursor of functional carbon attributing to two main aspects. From element perspective, the synthesized functional materials mainly composed of carbon element, and biomass is a carbon-rich material. Besides, other element such as H, O, N and S can be removal by thermal conversion to some extent [34]. Apart from C, O, H, S and N, biomass is also traceable some mineral substance such as, Ca, K, Mg, Na and Si [35]. For example, biomass which lives in saline-alkali land is rich in mineral element. What's more, the ratio of mineral elements in biomass is different depended on the biomass species or organs. These trace minerals can also play an irreplaceable role in the energy storage of biomass [35]. From another structure perspective, biomass possesses a comparatively stable three-dimensional framework, thus, its structure inherits original one after thermal pyrolysis for the removal of degradable composition [36]. The synthesis of activated electrode materials usually composes of carbonization and activation which can be completed in either two-phase or a single phase. The carbonization of a kind of biomass usually happens at temperature between 400 °C and 900 °C using nitrogen as protective gas. Activation is a process of transforming biochar into functional materials by pyrolysis at relative high temperature in a tube furnace or a microwave. Physical and chemical activation are the most common used to adjust pore structure and graphitization degree. Physical activation is consisted of two stages which carbonization at low temperature in a protective gas and activation at high temperature with using CO_2 or steam as activating agents. During a special activation phase, the biomass reacts with gas at high

temperature to form porous texture. Porous texture with hierarchical micro/meso/macro-pores can reduce the diffusion distance for electrolyte ions and decrease the electrical resistance of active biochar materials. Yoshizawa et al. prepared porous active carbon by physical activation means using coconut-shell [37]. In a conventional process, the coconut-shell was firstly carbonized under a nitrogen atmosphere and then the biochar was immersed in hydrofluoric acid and hydrochloric acid solution before being washed by deionized water. Subsequently, physical activation was taken place in carbon dioxide atmosphere at 900 °C. In spite of the physical activation method being fast, the pore formation by this means is not appropriate exactly and the specific surface area of active electrode material is not high enough. Furthermore, the physical activation consumed energy is quite more than that of the chemical activation. For chemical activation, it usually includes three stages: Firstly, the natural precursor is pyrolyzed at low temperature, then immersed in a chemical activating agents solution such as NaOH, KOH, $ZnCl_2$, H_3PO_4, heated in a protective atmosphere (e.g. N_2) at temperature that commonly ranging from 500 to 800 °C [38]. As a result, lots of channels and pores are formed in the carbon skeleton, which enable electrolyte ions transfer quickly and store efficiently [39]. Among chemical activating agents, KOH is the most generally applied in chemical activation. Wang et al. prepared celtuce leaves-based active carbon by KOH activated method [40]. The celtuce leaves were pyrolyzed at 600 °C for 1 h and mixed with KOH solution with optimized mass ratio. Then the product was activated in a furnace at high temperature and followed by washing with diluted HCl and deionized water. The activated carbon demonstrated a large specific surface area (3000 m^2 g^{-1}) than original celtuce leaves. When used celtuce leaves-based active carbon as electrode active material, it exhibited quite good electrochemical capacitance (421 F g^{-1} at 0.50 A g^{-1}). It is important that some species such as bagasse or corn stalk, can be directly pyrolysis into hierarchical porous materials without further activation, because the Ca, K, Na, and Mg salts naturally exist in these feedstock and can be used as activating agents. Generally, biomass can be classified into three main categories, the plant, microorganism, and animal remains. In below sections, we discuss biochar with excellent performance based on these three biomass species in detail.

2.1. Plant-based biomass

In general, plant or plant-based biomass is usually involved lignocellulose. It is mainly consisted of carbohydrate polymers such as cellulose, hemicellulose, and lignin [41]. However, the chemical compositions content is different from various plants organs. For example, seed teguments of arecaceae (coconut, areca-nut, etc.) contain percent of carbohydrate polymers as high as 65% [42], the bast plant (jute, hemp) normally have more proportion of cellulose (>50%) [43], wheat straw contains relative low cellulose ratio (31–44%) [44].

Cellulose, either direct utilization of commercial cellulose or extraction from biomass, can be employed to synthesize cellulose-based carbons for SCs electrodes [45,46]. Gleb et al. choose cellulose as carbon source to fabricate functional electrode materials, the as-prepared electrode demonstrated a specific capacitance of 236 F g^{-1} under sweep speed of 1 mV s^{-1} as well as high rate property [47]. A novel method recently has been widely applied that dissolving cellulose in alkaline solutions. Ma's group dispersed cellulose in the solution of NaOH/urea/H_2O with a certain proportion under stirring for 4 h at −8 °C. Micro/mesoporous carbon was successfully obtained by carbonization method without any activation for supercapacitors. During this process, the structure transformation from hard carbon to open interconnected pores is due to the pyrolysis of cellulose. The obtained electrode exhibited specific capacitances of 160 F g^{-1} at 0.2 A g^{-1} in 1 M H_2SO_4 solution. Symmetry supercapacitor has the very excellent cycle stability [48].

Lignin is also an alternative precursor for the electrode material in SCs [49]. In a typical biomass, lignin links between cellulose and hemicellulose. It mainly consists of 3 essential alcohol types: p-coumaryl, coniferyl, and sinapyl [50]. Part of heteroatom doping in the electrode material can enhance its wettability and pseudocapacitance. Lin et al. prepared lignin-based hierarchical porous carbon (LHPC) by a simple chemical activation method [51]. First, lignin was mixed with KOH solution and solidified. Then the mixture composites were calcined. The obtained LHPC consisted of a 3D network decorating with the hierarchical mesopores and micropores on carbon walls. Furthermore, LHPC had a good capacitance performance (165 F g^{-1} at 0.05 A g^{-1}) and outstanding cycling stability (97% over 5000s) when investigated as supercapacitor electrode. Hemicellulose is a major constituent in the cell wall of plant-based biomass. It is polysaccharide and mainly composed of glucose, arabinose, galactose and relative lower degree of polymerization compared with that of cellulose [52]. Wang et al. extracted hemicellulose from hemp stem by soaking in NaOH solution and filtrating with ethanol [53]. The extracted hemicellulose was treated hydrothermal reaction following chemical activation. The finally obtained hemicellulose-derived carbon samples exhibited excellent electrochemical performance, which is attributed to abundant micropores and oxygen functionalities.

2.1.1. Straw/stem of plant

Straw or stem of plant with long bundles shape conveys photosynthesis organics from leaves to all organs and assimilates water/salts from root. So the ion content is higher in straw or stem. To make straw or stem active carbon, carbonizing at high temperature is commonly employed [54–58]. Salt as additive agents can also play a crucial role in functional carbon forming. Jiang et al. prepared from low-cost, renewable biomass cornstalk under an air atmosphere (Fig. 1a). During the activation process, neutral salts (NaCl, KCl) were reacted as activate reagents [59]. Molten salt not only could prevent the cornstalk from burning, but also provide high concentration of Cl^- ions to etch the tissue and form micro- and meso-porous structures. The as-prepared materials exhibited ultra-thin sheets (thickness ~4.6 mm), large specific surface area (1588 m^2 g^{-1}), three dimensional layered framework. The electrochemical performance showed that cornstalk-based active carbon had excellent specific capacitance with 407 F g^{-1} and superior cycling life with 92.6% capacitance retention over 20000 cycles. Another alternative one is wheat straw [60]. This long fiber plant can be turned into nitrogen-doped three-dimensional network porous carbon by high temperature heating using melamine as nitrogen precursor. Nitrogen can modify the electron/donor property and decrease electrical resistance. The synthesized doped carbon material demonstrated comparatively superior specific capacitance of 275 F g^{-1}. Such outstanding electrochemical properties mainly are contributed to its three dimensional porous structure.

2.1.2. Leaf of plant

A leaf is mainly consisted of mesophyll tissues which provide nutrient substance for other organs through photosynthesis, so the percent of saccharides and protein in leaf are higher than that in other organs. The leaf includes a great deal of intrinsically oxide or nitrogen in a form of surface functional groups, which can embed of the leaves during pyrolysis and form porous structure in the active electrode material [61–65]. S/N-codoped hierarchically porous carbons was synthesized through ammonium nitrate (AN) activation of ginkgo leaf (Fig. 1b) [66], The relatively higher content of N and S compared to that in other biomass ensures that the ginkgo-derived porous carbons can be self-doped with N and S heteroatoms. It is believed that the use of AN generated large amounts of mesopores and micropores through chemical etching of the carbon skeletons, which promoted the formation of hierarchical pores. Consequently, assembled symmetric supercapacitor shows a high specific capacitance of 330.5 F g^{-1} at a current density of 0.5 A g^{-1} and an excellent capacitance retention of 85.8% after 10 000. Other leaf-based carbon can also be interconnected to fabricate a three dimensional structure. As an example, Liu et al. prepared microporous

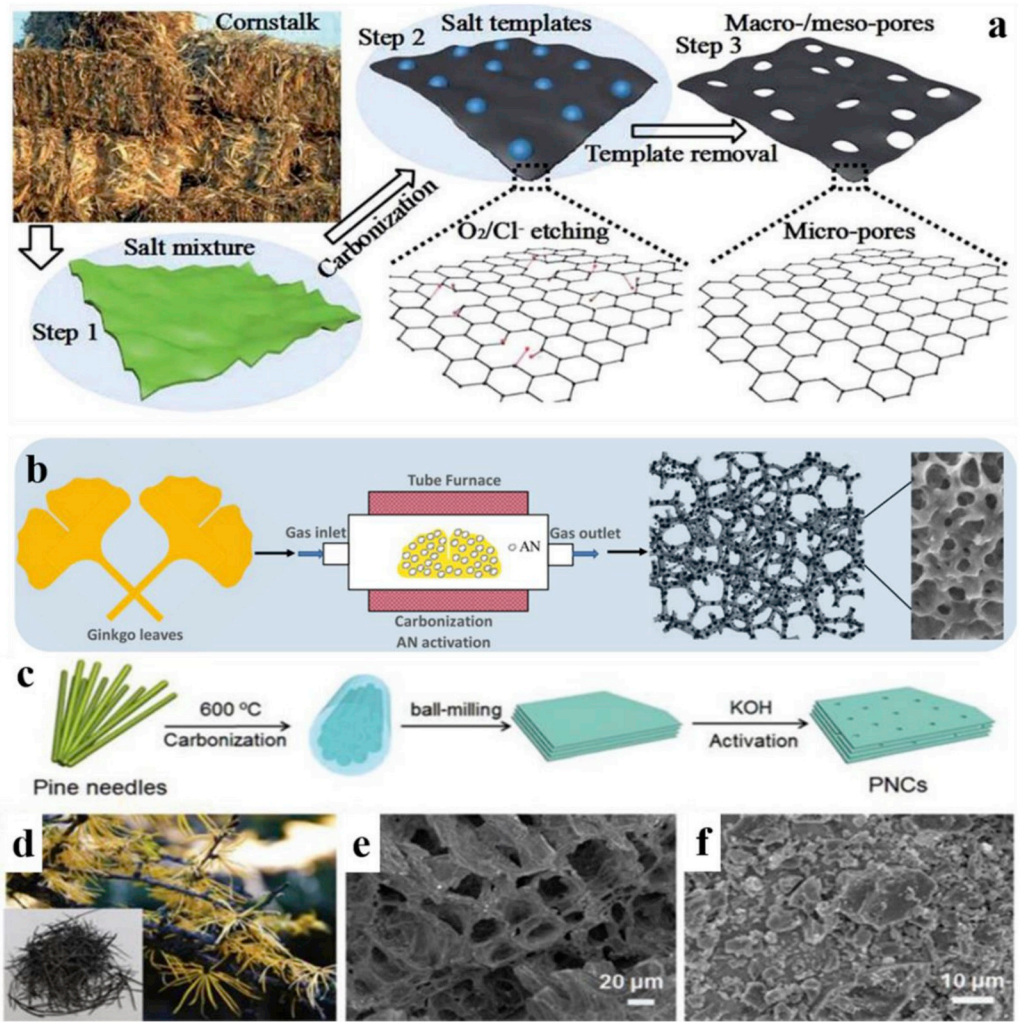

Fig. 1. (a) Schematic illustration of the macro/mesopores structure from cornstalk under an air atmosphere. Reproduced with permission from Ref. [59] copyright 2018, Royal Society of Chemistry. (b) Scheme illustrating the synthesis of ginkgo leaf-derived hierarchically porous carbon. Reprinted with permission from Ref. [66], Copyright 2019, American Chemical Society. (c) Schematic illustration of the synthesis porous carbon from pine needles. (d) Photo of raw pine needles. SEM images of activation at (e) 600 °C. (f) 900 °C. Reprinted with permission from Ref. [67], Copyright 2017, Royal Society of Chemistry.

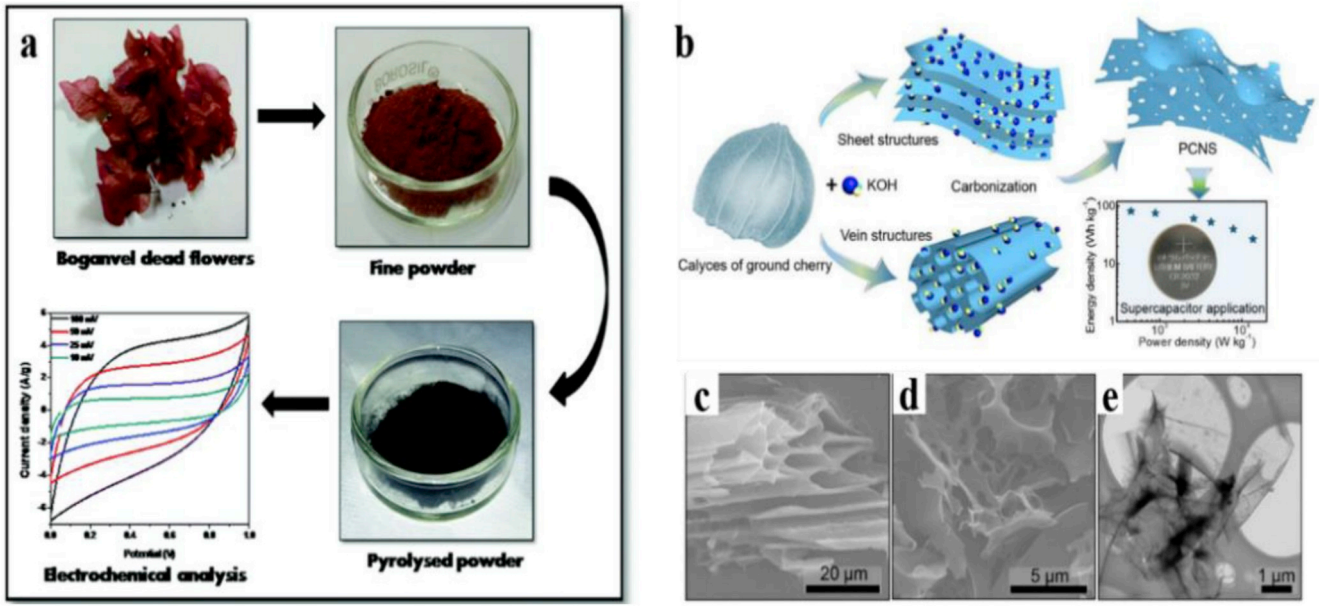

Fig. 2. (a) Schematic illustration of the perforated graphene from bougainvillea flowers. Reprinted with permission from Ref. [74], Copyright 2018, Royal society of chemistry. (b) Schematic illustration of the synthesis and supercapacitor applications derived from calyces of ground cherry (GCC). (c) SEM images of the GCC by direct carbonization process. (d) (e) SEM and TEM image of GCC after activation process. Reprinted with permission from Ref. [75], Copyright 2018, Wiley.

functional material through carbonization and KOH activation using pine needles as precursor (Fig. 1c) [67]. The resulted carbon has considerably interconnected pores with the size between 0.5 nm and 2 nm, high specific surface area of about 2433 $m^2 g^{-1}$ (Fig. 1d, e, f).

What's more, the leaf-based active electrode materials by KOH activation can also be synthesized based on lotus leaves [68], celtuce leaves [40], indicalamus leaves [69], mulberry leaves [70], corn leaves [71] and so on.

2.1.3. Flower of plant

The dry flowers mainly possess saccharides, protein, glucosides, vitamin in petal [72,73]. In addition to organic components, calcium and magnesium are existed in some flowers. These metal salts can be used as template to produce pores of activated electrode material. An example for bougainvillea flowers, Kale et al. prepared perforated graphene through carbonization without additional activating reagents (Fig. 2a) [74]. The fabricated active carbon demonstrates specific surface area of 850 $m^2 g^{-1}$. The assembled supercapacitor displays a high electrochemical capability of 458 F g^{-1}, long cycle life over 10 thousand cycles, and high energy density of 64 Wh kg^{-1} at power density of about 273 Wh kg^{-1} in alkaline aqueous electrolyte. The part of covering flowers are lantern-like calyces which major ingredients of cellulose and proteins. Interestingly, there are distinctive microtubes of thin sheets. As reported by Yu, a three dimensional structure with carbon nanosheets has been fabricated from ground cherry calyces successfully, which consisting transparent sheet with a number of hollow vascular structures (Fig. 2b, c, d, e) [75].

2.1.4. Seed of plant

There is a kind of plant in the natural world whose seeds are flocculent and can be spread to distant places with assistance of wind, such as catkins, poplars and dandelions. The morphology of these seeds is hollow and thin-walled tubes, which can be used as an ideal precursor of active porous materials [76–81]. Carbon tube covered with hierarchical pores is successfully prepared using dandelion fluff as precursor [82]. The porous framework lead to quick charge convey aside the tube wall or electrolyte ion transmit inside tubes (Fig. 3a and b). Benefiting from hollow bundles, the electrode shows quite superior energy density of 12 Wh L^{-1} at power density of 700 W L^{-1}. Adding heteroatoms with active carbon is important to optimize its electron-donor properties and improve wettability consequently improve performance of their surface. Yan et al. used Thiourea (CN_2H_4S) as both the N and S source to prepare willow catkin-derived hierarchical porous nanosheets (Fig. 3c and d) [79]. The EIS measurement showed relaxation time of dual-doped sample decreased 2.13 s compared with control sample. Therefore, the enhanced ion diffusion is favorable for rate performance at higher charge-discharge rates.

2.1.5. Fruit of plant

The fruit possibly is different from the chemical compositions in regard to the variety and parts. Nevertheless, it also has a part of the same components such as moisture, protein and lipids. The protein and lipid included in the fruit pulp are account for 6%–43% [83]. Such high percentage of protein and lipid offers relative low contribution to the carbon in the pyrolysis process, because these organics decompose at temperature below 300 °C, letting out volatile substances such as CO_2, H_2O, NH_3, etc. So hydrothermal carbonization (HTC) is common to convert pulp into coal-like materials under mild conditions [84]. Compared to physical or chemical activation, HTC is completed at relative low temperature (100–250 °C). It is inspired by coaling process that coal is transformed from biological materials through thousands or millions of years. However, the HTC-based biochars show less pores and low surface area, which don't meet the need for the energy storage field. Additives or templates can increase the channel and surface area of HTC-based active energy materials. For example, a kind of porous carbon has been prepared derived from waxberry through hydrothermal reaction and pyrolysis [85]. During the HTC process, $Fe_2(SO_4)_3$ does not only provide S element but also influence the morphology of the solid

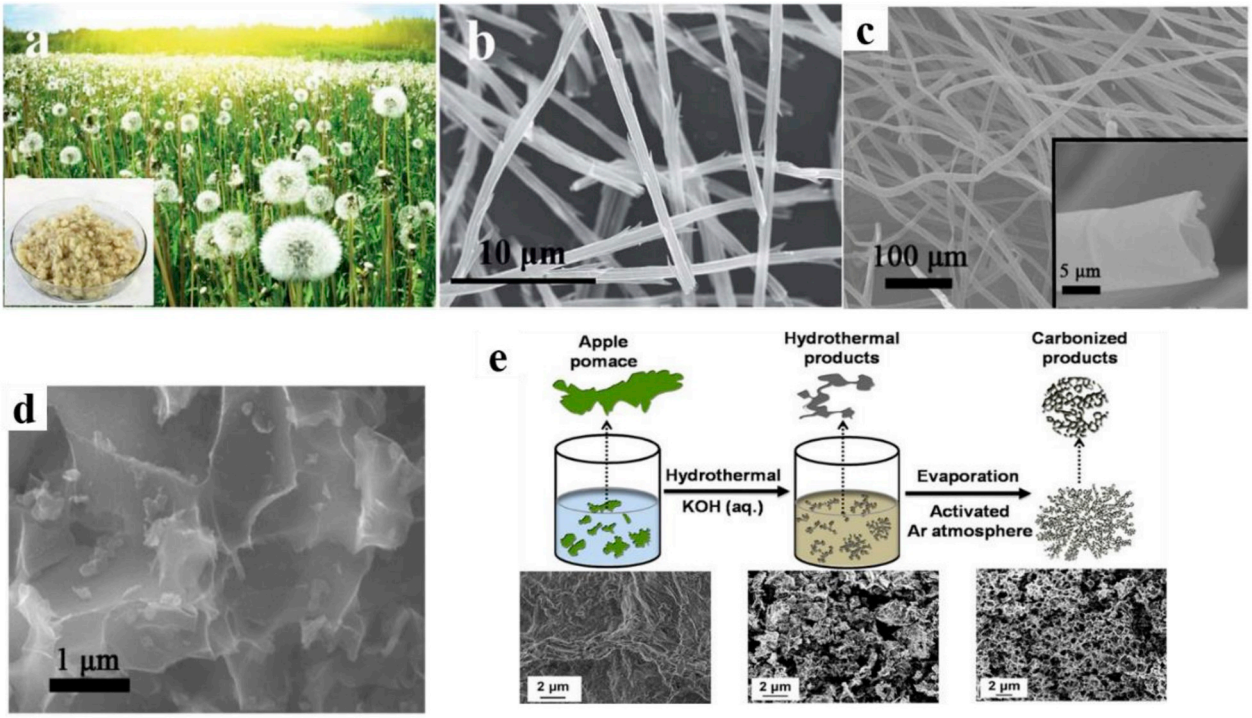

Fig. 3. (a) Photographs of the dandelion. (b) SEM images of the resulted hollow microstructures. Reprinted with permission from Ref. [82], Copyright 2017, Royal Society of chemistry. (c) The SEM image of willow catkin. (d) The SEM images of N, S-PCNs1-1. Reprinted with permission from Ref. [79], Copyright 2016, Elsevier. (e) Schematic illustration of the preparation of apple pomace derived carbon materials. Reprinted with permission from Ref. [87], Copyright 2018, American Chemical Society.

products (from nanosheet to microsphere). The electrochemical measurement result exhibits outstanding capacitive performance (1320.4 F cm^{-3} at 0.1 A g^{-1}), good cycle stability (>50 000 cycles), and superior energy density (101 W h kg^{-1} at 222 W h L^{-1}). Edward et al. obtained activated carbons produced from two different fruit dehydration wastes (blueberry and cherry) through hydrothermal carbonization and chemical activation method [86]. Shen et al. used apple pomace as a feedstock to prepare active carbon materials through a hydrothermal and activation means [87]. The achieved samples demonstrate a 3D flatty porous framework with the diameters about 500 nm (Fig. 3e). The porous frameworks can simultaneously offer effective route and accessible surface to electrolyte ions.

Fruit peels are known as the by-product, most of them are straightly discarded or burned, which give rise to resource waste as well as result to environmental contamination. The fruit peel is composed of fiber and saccharides, which can be considered as the feedback to synthesize activate carbon materials [88–93]. This is a clean and renewable method to deal with the abandoned waste. Many kinds of fruit peel such as banana peel [94], pomelo peel [95], peanut shell [96], garlic skin [97] and lotus seed shell [98] have been successfully turned into active carbons by chemical activation method. For example, Li et al. reported honeycomb-like structure carbonaceous materials by the combination hydrothermal carbonization with chemical activation using pomelo peel [99]. Such carbon material showed high level of graphitization, relatively small quantity of micropores/macropores and a specific capacitance of 374 F g^{-1}. Han et al. activated longan shell to be idea electrode material with large surface area of 3260 m^2 g^{-1} and superior electrochemical capacitance of 322 F g^{-1}.

2.2. Microorganism-based biomass

Besides plants, biomass-based active carbon can also be prepared using microorganisms as precursor, such as bacterial cellulose. In their growth process, the hyphae of microorganism interconnect to form a 3D network, which makes tissue transform shape into a honeycomb-like structure and provides an effective way for the development of unique hierarchical structure [100]. The chemical compositions of microorganisms include carbohydrates, proteins, fibers, fat, and ash [101]. The carbohydrates of the microorganism are mainly chitins, which are interconnected and can acted as a major carbon source in high temperature carbonization [102]. Fungus, a kind of widespread eukaryotic organisms, can use as an alternative carbon source. In 2014, Long et al. used fungus to prepare nanosheet active carbon by hydrothermal method and subsequent carbonization process for the first time [103]. In the process of hydrothermal, KOH is added and acted as template that preventing cell walls from agglomeration. In the meantime, KOH can serve as activating reagent for the fabrication of porous structure. As a result, the as-prepared active carbon shows superior electrochemical capacitance of 360 F cm^{-3} and a good cycle life (99% capacitance retention over 10000 cycles). Mushrooms are also a kind of promising source to prepare active carbons in the variety of microorganism-based biomass. Ogale et al. have found plenty of cross-linked carbon nanosheets with curtain-like frameworks synthesized from mushroom via hydrothermal and activation method [104]. The fluffy plicate and laminate carbon nanosheets formed a cage-like structure, which can serve as ion-buffering reservoirs to improve ion diffusion in the charge/discharge process. Tremella is also a type of general and priceless fungus. Han et al. used it as a precursor to achieve the transforming of its wire-like compounds into 3D layered porous active material via facile hydrothermal and chemical activation method (Fig. 4a) [105]. Bradyrhizobium japonicum is a kind of microorganism which has symbiosis relationship with soybean roots. Significantly, it includes sufficient nitrogen (about 6–10 wt%), which can be considered as an available resource in preparing N-doped active energy materials [106]. Sun et al. prepared N-doped three dimensional structure active carbon based on Bradyrhizobium japonicum in energy storage field by carbonization and subsequent $ZnCl_2$ activation (Fig. 4b) [107]. The obtained active electrode materials exhibit large specific surface area (1275 m^2 g^{-1}),

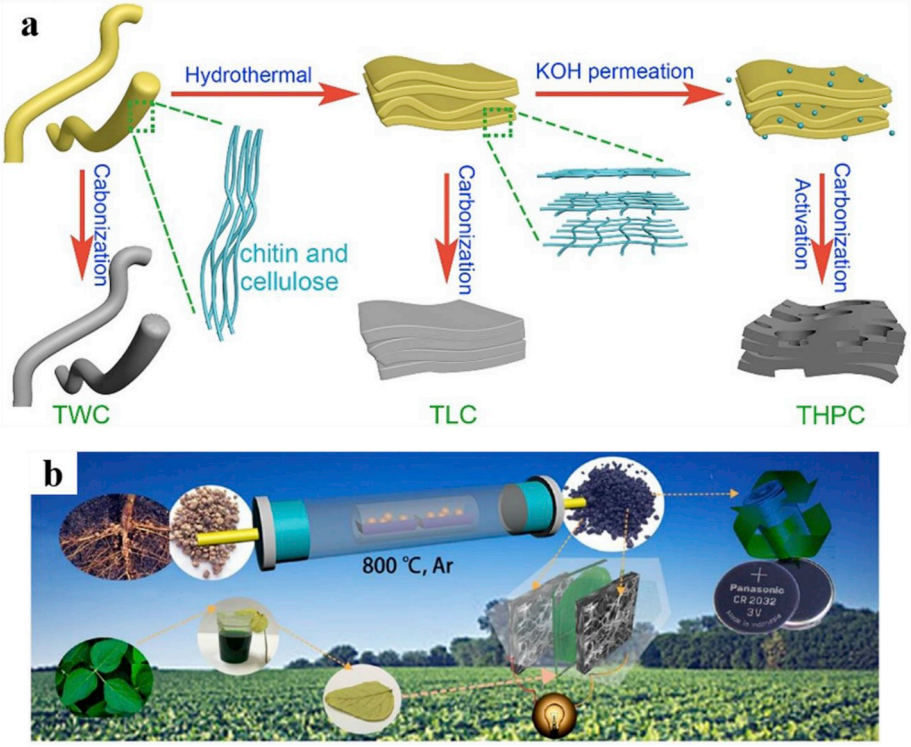

Fig. 4. (a) Schematic illustration of the preparation of tremella-based sheet-stacking flatty porous carbon. Reprinted with permission from Ref. [105], Copyright 2018, Elsevier. (b) Schemetic of the preparation of porous structure carbon derived from Bradyrhizobium japonicum. Reprinted with permission from Ref. [107], Copyright 2018, American Chemical Society.

hierarchical porosity structure and outstanding electrical conductivity.

2.3. Animal remains-based biomass

A great deal of animal and their metabolin, such as insects, mollusks, and crustaceans can be acted as the original resources in the production of biomass-derived carbon [108–113]. Chitin, as one of the most abundant polysaccharides, is mutual chemical composition in form of chitin nanofiber [39]. Importantly, large proteins and aliphatic acids constituent also facilitate the considerably active carbons incorporated with doping element. Xu et al. reported egg yolk-derived active carbons with loose spongy structure using $C_3N_3Na_3S_3$ and KOH as dual activators (Fig. 5a and b) [114]. Based on a series of electrode samples, they found structural parameters have an impact on electrochemical properties. The percent of micropore area (S_{micro}/S_{BET}) can coincidently influence all performances including specific capacitance, power density, energy density and rate capability with the same tendency. So that S_{micro}/S_{BET} is expected to be one composite performance indicator to reflect the

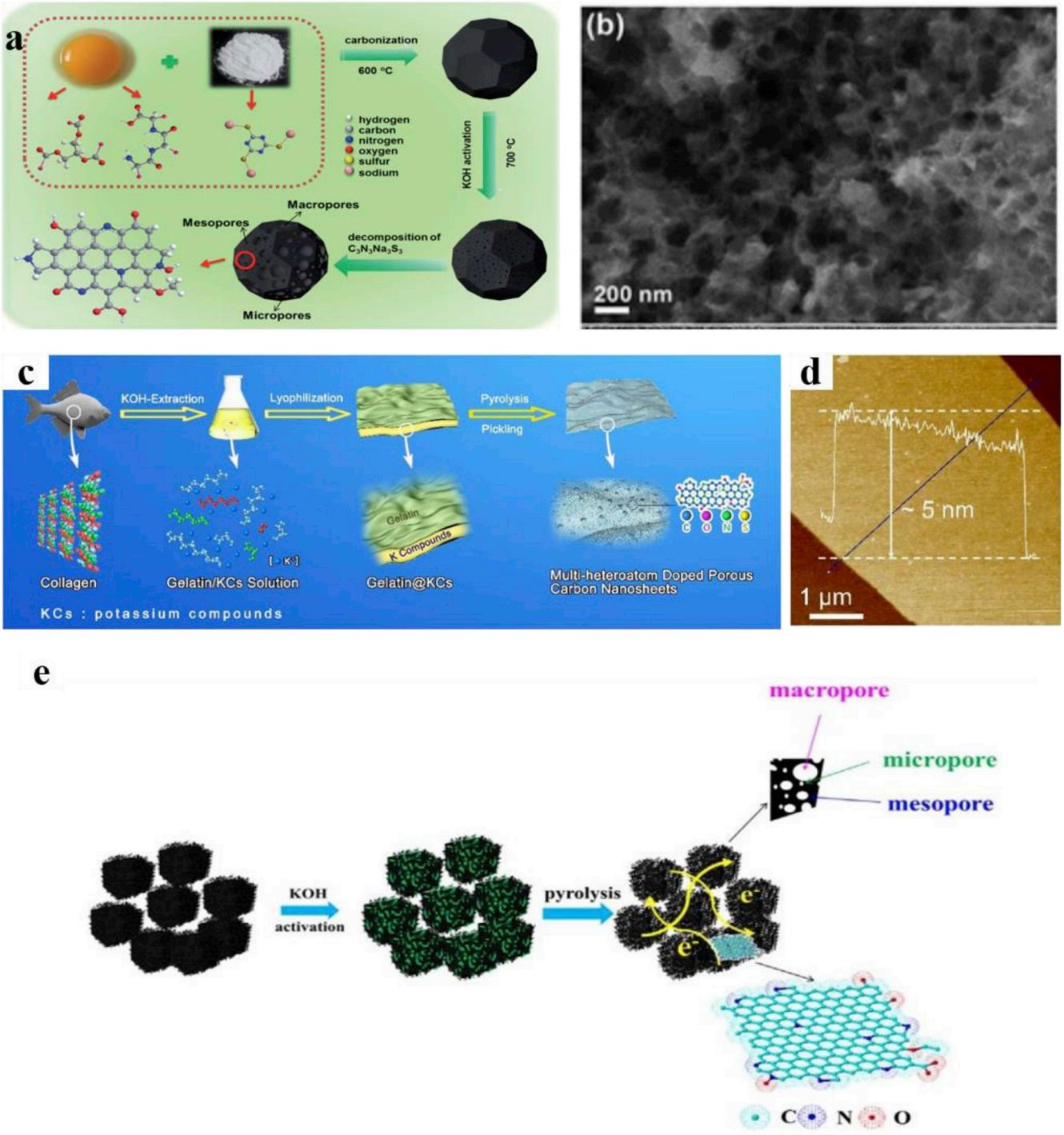

Fig. 5. (a) Schematic illustration of the production processes for the 3D flatty porous carbons from egg yolk. (b) SEM image of egg yolk-derived active carbons. Reprinted with permission from Ref. [114], Copyright 2018, Elsevier. (c) Schematic illustration of the preparation of thin layered carbon doped by O, N and S element from fish scales. (d) AFM image of fish scales-derived active carbon. Reprinted with permission from Ref. [115], Copyright 2018, Elsevier. (e) Schematic illustration of N/O-coped porous carbon derived from pigskin. Reprinted with permission from Ref. [116], Copyright 2018, Elsevier.

structure–function relationship. Wang and cooperator employed fish scale as precursor to synthesize multiple heteroatom (N, O, S) doped thin layered carbon [115]. It has porous nanosheet framework (thickness of 3–5 nm), large micropore ratio, rich surface heteroatoms, empowering the electrodes with excellent electrochemical properties (Fig. 5c and d). Dunmin et al. have prepared a pigskin-based hierarchical active energy material with effective active sites by a simple high-temperature pyrolysis process. The achieved samples possess three dimensional porous frameworks with large mesopore volume and heteroatom incorporated with nitrogen and oxygen, that result to high specific capacitance (Fig. 5e) [116]. Other animal-derived active electrode materials can also be fabricated from shrimp shell [117], human hair [118] and gelatin [119].

In summary, plant, microorganisms and animal remains can be considered as potential carbon precursors for SC electrode materials (Table 1). Selection of the biomass precursor for high-value activated carbons depends on several criteria such as intrinsic microstructure and composition. Recently, our group have used cotton stalk [120], cellulose [48], saussurea involucrata stalk, algae [121] and other long fiber precursors to obtain good surface morphology activated carbon for supercapacitor application. From structure perspective, long fiber biomass is featured with branch-like structures and stable three-dimensional interconnection networks, thus, it can subject to chemical or thermochemical treatment for the removal of its readily degradable constituents (all hemicellulose and most cellulose as well as partial lignin) [122]. As a result of the removal of those readily degradable constituents, many channels and uniform pores are formed in the active carbon material after simple chemical activation method. Based on its abundant channels and pore structure, long fiber biomass-based carbon provides more entrance pathways for electrolyte ions and assists the expansion of active mass volume during cycling, which is considered to be an ideal sample for energy storage applications. For instance, Ma et al. reported flute shape micropores electrode material based on cotton stalk in supercapacitors [120]. The as-prepared carbon with many micropores showed large specific surface area (1964 $m^2\ g^{-1}$), opened pores, 3D interconnected network, appropriate graphitization degree, which could not only decrease transfer distance for ion or electron but also increase the effective specific surface area. From composition perspective, long fiber biomass has principal component of lignocelluloses, and small amounts of simple sugar, protein, starches and lipids. Lignocellulose can be easily altered into nano-sized fiber owing to the presence of elemental fibril (diameter of 2–5 nm) of the cellulose linked by covalent linkages and hydrogen bond [123]. To date, several techniques (pyrolysis, hydrothermal treatment) have been employed to remove the linkages in order to create carbon nanofiber with different surface morphologies. Therefore, producing activated carbon from long fiber biomass displays many advantages such as hydrophilicity, high surface and aspect ratios, excellent mechanics and flexibility, which make it appropriate electrode with superior electrochemical properties.

Table 1
The electrochemical properties and relevant structural factors of biomass-based carbon derived from plant-, microorganism- and animal remains-based raw material.

Precursor	Activation	SSA ($m^2\ g^{-1}$)	C (F g^{-1})	Current density (A g^{-1})	Rate performance
Lotus stem [124]		1610	174	0.5	80% at 20 A g^{-1}
Wheat Straw [60]	$CaCl_2$	892	275	0.2	81% at 8 A g^{-1}
Cornstalk [59]	NaCl, KCl	1588	407	1	60% at 20 A g^{-1}
Rice straw [125]	KOH	1122	337	1	83% at 20 A g^{-1}
Cotton stalk [120]	KOH	1964	254	0.2	87% at 20 A g^{-1}
lotus receptacle [126]		1015	340	0.5	67% at 20 A g^{-1}
Bougainvillea flowers [90]		850	458	2.28	22% at 5.8 Ag^{-1}
Rose [127]	KOH	1911	208	0.5	52% at 20 A g^{-1}
Perilla frutescens [128]		655	270	0.5	75% at 20 A g^{-1}
lotus leaf [68]	KOH	2488	379	1	79% at 20 A g^{-1}
Celtuce Leaves [40]	KOH	3404	421	0.5	62% at 10 A g^{-1}
Macadamia Nut Shell [129]	KOH	2806	231	1	39% at 10 A g^{-1}
Rice husk [130]	KOH	3120	315	0.1	60% at 50 A g^{-1}
Coconut shells [29]	K_2CO_3	1506	91.15	0.2	89% at 2 A g^{-1}
Tremella [105]	KOH	1097	299	0.5	84% at 20 A g^{-1}
fish scale [115]	KOH	962	306	1	78% at 200 Ag^{1}
Chinese human hair fibers [118]	KOH	1306	340	1	67% at 10 A g^{-1}
egg yolk [114]	KOH		549	1	52% at 30 A g^{-1}

3. Structure of biochar and electrochemical performance

It is widely believed that the carbon materials mainly relied on electrical double layer capacitors to achieve energy conversion. Which depend on the electrostatic adsorption/desorption of ions in the energy storage materials. Hierarchical porous materials can improve energy storage capacity [131–133]. So far, various biomass, have been extensively employed as feedstock to fabricate hierarchical active carbons by carbonization and further activation method. On the one hand, porous frameworks are inherited from the frameworks of the plant which is beneficial for obtaining necessary water and ions in surroundings. These pores of raw biomass may be maintained in fabrications of active energy storage materials. On the other hand, raw biomass is generally consisted of organic substances like saccharides, vitamin, fatty acids. In the process of thermally pyrolysis or carbonation, a great deal of organic substances will be decomposed into H_2O and CO_2, and finally come out to leave pores [134]. More importantly, biomass-based active carbon can also be prepared through mixing some activating agents [135]. To achieve high-performance supercapacitors, researchers have make efforts to optimize the pore structure, modify the surface property and adjust graphitization degree.

3.1. Pore structure

Biomass materials generally show very multiple dimensions for macrostructures. Biomass-derived active carbon can be perfectively maintained or formed unique frameworks, such as spherical, tubular, honeycomb or graphene-like carbon. The electrochemical performance of supercapacitors probably increases with specific surface area, but the function is diversified. Pore framework (porosity and size distribution) is another important factor on energy storage power of active energy materials in supercapacitors. Macropores (>50 nm) can act as ion buffering reservoirs, decreasing convey distances from electrolyte to electrode. Mesopores (2–50 nm) can offer channels for the charge transfer. Micropores ensure high specific surface erea and contribute electrical double layer capacitance. Currently, efforts have paid to fabricate hierarchical porous carbon with different dimension through adjusting experimental parameters such as activation reagent amount [114,136–138], activation temperature [29,139–142], activation reagent type [143–148]. Ma's group reported a highly ordered micropores

activated carbon can be observed from cotton stalk [120]. By altering the proportion of KOH/C, highly ordered micropores activated carbon (HOMAC) materials was obtained when KOH/C is equal to 4. This active carbon shows a high capacitance (322 F g^{-1}) and energy density (33.91 W h kg^{-1}) in the diluted H_2SO_4 solution. Cui and cooperators developed a three dimension porous carbon aerogel using prolifera-green-tide by pyrolysis and subsequently chemical activation [149]. By changing activation temperature, the ratio of macro/meso/micropores can be regulate correspondingly. Under optimized conditions, the active electrode material possesses large accessible surface area of 2200 m^2 g^{-1}. It shows electrochemical capacitance of 260.6 F g^{-1} and good structure stability (92% capacitance retention over 10 thousand cycles) in two electrode system using aqueous electrolyte. Apart from activating raw biomass by using KOH, some other activating agents, such as $CaCl_2$, NaCl, $ZnCl_2$, KCl, K_2FeO_4 and H_3PO_4 were also used for the activation process. Lee and cooperators explored the relationship between electrochemical properties and structure of active carbon designed by different activating reagents (KOH, $ZnCl_2$ and H_3PO_4) [150]. The results show the distribution of pores on the surfaces was strongly influenced by the activation agent. The pores on the surface of sample activated by KOH are mostly large, open and hierarchical. The pores on the surface of sample activated by $ZnCl_2$ are not clearly visible. Samples which the surface of sample activated by H_3PO_4 show large cavities in which small pores are embedded.

The pore framework of carbon can be demonstrated as zero dimension (0D) to three dimension (3D) to facilitate ion diffusion. Active material with various pore size in 0D, 1D, 2D and 3D is benifitial for supercapacitors because of its minimizing ion transport distance. Recently, a diverse structures of carbon materials have been developed, such as 0D nanospheres or hollow structure; 1D nanofibers or nanotubes; 2D nanosheets and 3D porous framework.

3.1.1. 0D nanospheres activated carbon

0D activated carbon nanospheres (ACNs) are a kind of popular carbon electrodes on account of its large accessible area, low cost and high charge capacity. The diameter of the biomass-based spheres is ranging between 50 and 500 nm and 1–5 μm. Yan and cooperators found that carbon sphere was successfully prepared using oatmeal as precursor by hydrothermal and followed carbonization method, showing glossy surface of spheres with about 2 μm diameter [151]. Gaddam and cooperators discovered that carbon sphere within small size was prepared using coconut oil through fire deposition [152]. The as-prepared carbon spheres exhibited diameter size ranging from 40 nm to 50 nm, relative low accessible surface area of 56 m^2 g^{-1}, which is applied in field of energy storage. Rufford et al. fabricated active carbon with a greater surface area (2871 cm^2 g^{-1}) and pore volume (0.81 cm^3 g^{-1}) by

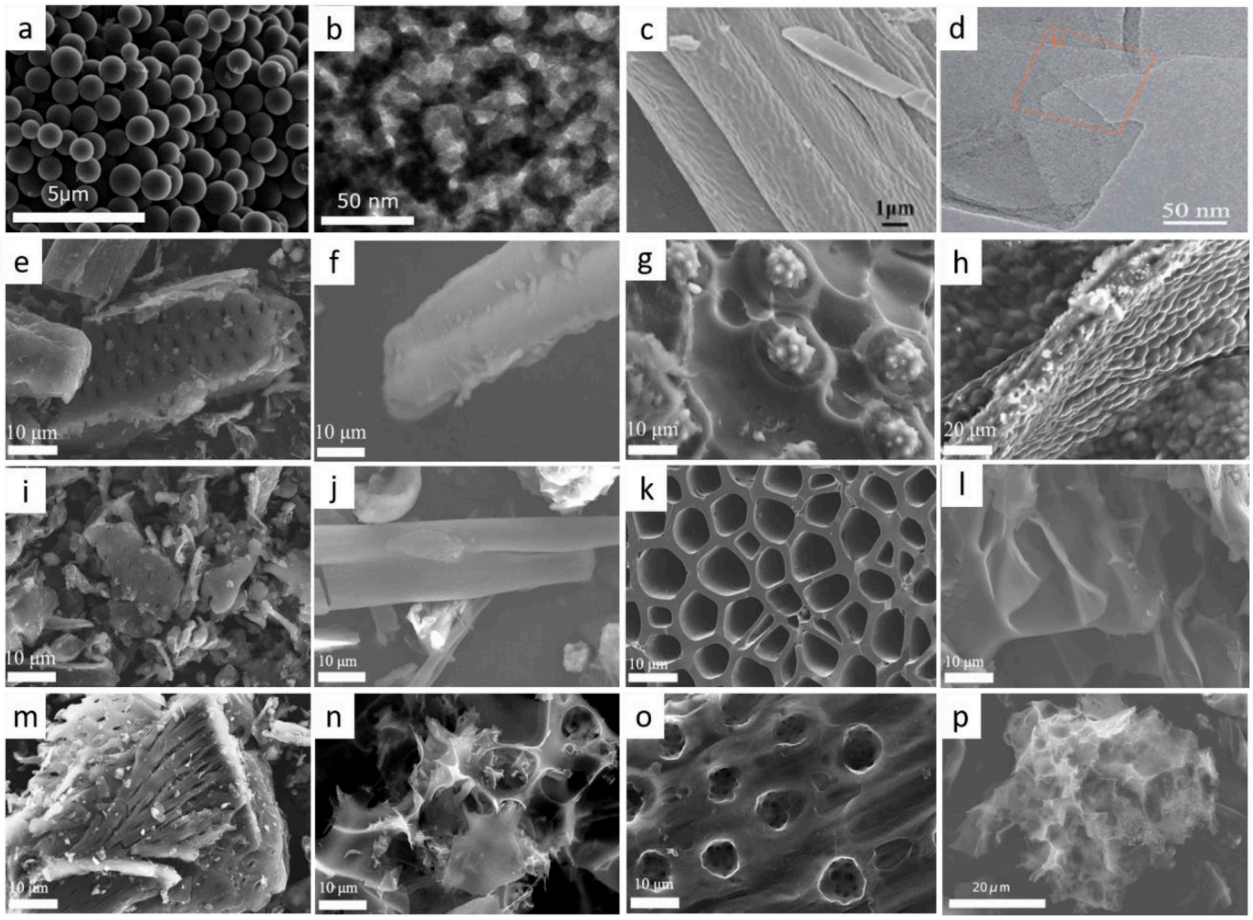

Fig. 6. SEM image (a) and TEM image (b) of porous carbon spheres derived from fermented rice. Reprinted with permission from Ref. [154], Copyright 2014, Royal Society of Chemistry. (c) SEM image of tubular structure of dandelion-based active carbon. Reprinted with permission from Ref. [156], Copyright 2017, Wiley. (d) TEM images of porous graphene-like nanosheets derived from coconut shell. Reprinted with permission from Ref. [91], Copyright 2013, Royal Society of Chemistry. The SEM image of cotton stalk (e), cotton stalk after carbonization (i), cotton stalk after activation (m). Reprinted with permission from Ref. [120], Copyright 2017, Elsevier. The SEM image of saussurea involucrata stalk (f), saussurea involucrata stalk after carbonization (j), saussurea involucrata stalk after activation (n). The SEM image of coconut shell (g), coconut shell after carbonization (k), coconut shell after activation (o). The SEM image of algae (h), algae after carbonization (l), algae after activation (p). Reprinted with permission from Ref. [121], Copyright 2019, Royal Society of Chemistry. Fig. 6f, g, n, j, k, o are all our group works, not published.

activation sugarcane bagasse using $ZnCl_2$ activator. It shows specific mass capacitance of 109 F g^{-1} and retains of 77% over 10 thousand cycles [153]. However, solid spheres are not beneficial to the transport of charge and the diffusion of electrolyte ions during electrochemical behavior. As a result, hollow carbon spheres have been attained much interest. Gao et al. prepared hollow carbon spheres with large SSA (2106.0 m^2 g^{-1}) as well as large pore volume (1.1 cm^3 g^{-1}) using fermented rice as precursor [154]. That specially opened framework in carbon spheres is related to chemical activating reagent $ZnCl_2$, which largely quicken transfer rate for ion from electrolyte into electrode (Fig. 6a and b). This electrode material presents excellent electrochemical properties in supercapacitors that capacitance of 219 F g^{-1} at a high current density of 15 A g^{-1} and superior cycling stability for after 4000 cycles. In generally, the interlinked hollow carbon spherical framework can provide an open and continuous ion diffusion and large effective surface area to ensure sufficient active sites for charge/discharge process.

3.1.2. 1D nanostructure carbon

Differing from 0D structures, 1D structures possess a relative higher aspect ratio that benefic for increasing surface area. Recently, carbon nanofibers and nanotubes were commonly employed in various electrode materials. Electrospinning is a simply method to design carbon nanofiber within small size (<100 nm). Some researchers utilize lignin as precursor to prepare biomass-derived carbon nanofibers via electrospinning technique. In general, electrospinning is composed of capillary tube, power supply and collector device. With regard to fabrication of biomass-based carbon nanofiber, the raw biomass is immersed by reagents to design fiber, then mixing the fiber with polymer solution uniformity in capillary tube. The size of carbon nanofiber can be adjusted by the operating potential, flow velocity, solution volume and length from nozzle to collector device. There are plenty of researches about together biomass with polymers in synthesis of carbon nanofiber with cross-linked porous framework. The polymers improve the viscosity of fiber solution during electrospinning process. Cross-linked porous framework can be applied as an open path during ion diffusion that can increase electrochemical performance. Tao et al. reported that walnut shell has been liquefied by phenol for 1 h, then polyvinyl alcohol was added into the colliquative solution previous to electrospinning process [155]. Polyvinyl alcohol had performed an effect of increasing fluid performance of the colliquative solution, generating carbon nanofiber with small diameter about 280 nm. Hence, it was clearly showed that the property of active carbon using electrospinning method can be improved by mixing with polymer solution. As a result, a superior specific capacitance of 380 mA h g^{-1} at 0.03 A g^{-1} as well as outstanding cycling life (above 280 mA h g^{-1} specific capacity over 200 cycles at 0.1 A g^{-1}) had been obtained from walnut shell/PVA carbon nanofiber. Carbonization can be employed to prepare interconnected carbon nanofiber. Liu et al. fabricated porous nanofibers with a diameter of tens of nanometers using renewable lotus seedpods as precursor via carbonization and activation process [131]. The assembled supercapacitor in two electrode system exhibited a prominent energy density of 13 Wh kg^{-1} at power density of 260 W kg^{-1}. Furthermore, tubular active energy materials can offer a continuous and open charge transportation pathway. A good deal of biomass source has hollow framework, such as dandelion, willow catkins, and cotton. Which be employed as feedback to fabricate conductive carbon nanotubes. Based on the reported paper, cotton fibers could well reserve porous hollow carbon nanotubes during heat temperature pyrolysis and chemical activation. The tubular active energy materials within few millimeters of length provide short-distance ionic pathway. At the same time, a great number of nanopores on the tube walls facilitate ion diffusion traversing the walls as well as increase accessible area for charge accumulation. In addition, poplar and willow catkins present porous tubes after pyrolysis. The raw dandelion is tubular [156]. The tubular framework of dandelion can be perfectively retained after carbonation, which effectively increase contact area with ions in the electrolyte (Fig. 6c). The hollow carbon tubes with porous structure are arriving at length ranging from 20 to 50 μm, and these hollow carbon tubes are interconnected. All in all, either 1D nanofibers or tubular framework offers a route for transferring charges and minimizing the ion diffusion path during electroactive process.

3.1.3. 2D graphene-like carbons

High temperature decomposing biomass into 2D graphene framework has currently considered as an effective route to promote electrochemical properties. The unique structure guarantees short ion transport, enabling biomass-based 2D graphene-like carbons as promising energy storage materials (Fig. 6d). Long et al. achieved ultrathin graphene-like active materials using auricularia by a hydrothermal method and a following pyrolysis process [103]. The specific surface area of graphene-like active carbon was 1103 m^2 g^{-1} and mass density was around 0.96 g cm^{-3}. That designed material displayed high capacitance of 360 F cm^{-3} as well as kept 99% of original one over ten thousand cycles. What's more, the assembled energy storage device based on same as-prepared electrodes showed an energy density of 22 W h kg^{-1}, cycle stability with 96% capacitance over 10 000 cycles, and a volumetric energy density of 21 W h L^{-1}. Layer stacked active carbon was prepared from cornstalk biomass via a $K_4[Fe(CN)_6]$ catalyzed pyrolysis method [157]. Wang et al. has currently designed graphene-like carbons using hemp bast fibers as precursor. They possess multi-level lamellar framework containing of cellulose and lignin. The diameter of hemp bast fibers are between 10 nm and 30 mm. The wall is made up of three layers. The hemp has the inherent feature of being quite interconnected in two dimensions, endowing the chance of extracting large thin carbon flake, which can be further linked in carbonization and activation. Zheng et al. fabricated 2D ultrathin carbon materials with a good electrochemical properties using glucose as a precursor [158]. In the course of chemical activation, potassium hydroxide used as an activating agent as well as a template to synthesis the 2D thin layered structure. The as-prepared carbon material showed an electrochemical capacitance of 257 F g^{-1} at 0.5 A g^{-1} as well as remained 72% capacitance at high current density of 100 A g^{-1}. Such high percent of micropores and low mesopores lead to large accessible surface area of around 2600 m^2 g^{-1}, which highly increase electrochemical capacitance. That interconnected thin layered frameworks quicken ion diffusion, so providing comparatively high rate capacity.

3.1.4. 3D hierarchical porous carbon

It is believed that the supercapacitors are achieved charge accumulation on the contact surface between the electrode and electrolyte, so they commonly own high power density and superior cycling life. The general disadvantage is their inferior in term of energy density. Hierarchical carbon has been seen as an ideal energy storage material on account of its outstanding conductivity, chemical stability, green initiative, and low cost. Nevertheless, the power capability of ordinary porous carbon materials is degraded by their unbefitting and blocked pore structure. Which result in poor availability for electrolyte ions under high current density. 3D flatty porous materials with large accessible surface area and appropriate porosity can effectively improve electrochemical behaviors in supercapacitors. Feng and cooperators developed a straightforward technique for preparation of polyporous structural active energy materials through hydrothermal method and subsequently chemical activation utilizing bagasse wastes as source. The obtained bagasse-based porous carbon displayed connected network and appropriate porosity, owning a accessible surface area of 2296 m^2 g^{-1}. The assembled supercapacitor demonstrated a specific capacitance of 320 F g^{-1} at 0.5 A g^{-1} and 71% capacitance retention at 50 A g^{-1}. Hao and cooperators synthesized 3D flatty active energy materials employing bagasse as raw precursor [159]. Solid state supercapacitor was designed in and because of characteristics of open porous framework, quite outstanding specific capacitance of 142 F g^{-1} at 0.5 A g^{-1} was

reached. Furthermore, as-prepared solid state supercapacitor showed high rate capability and capacitance retention of 94% after 5000 cycles. Fan et al. synthesized 3D flatty honeycomb-like active material via a simple pyrolysis of KOH immersed wheat flour [135]. Such hierarchical porous framework, large surface area (1313 m^2 g^{-1}) ensure the active energy materials to display a superior specific capacitance of 473 F g^{-1} at 0.5 A g^{-1} using 6 M KOH as electrolyte. Recently, we analyze activated carbon derived from four kinds of long fiber biomass. The precursor is cotton stalk, saussurea involucrata stalk, coconut shell, algae, respectively. Their structure at different pyrolysis stage is compared systematically. Fig. 6e–h shows the initial structure of the cotton stalk, saussurea involucrata stalk, coconut shell and algae. There are many pores with a diameter of about 2 μm in the cotton stalk. Saussurea involucrata is a fibrous structure with a high aspect ratio. The coconut shell exhibits a long fiber with dense particles distributed on its surface. The surface of algae is flaky and rough. After carbonization, the structure of these four materials was shown in Fig. 6i-6l. The morphology of cotton straw and saussurea involucrata stalk did not change significantly. This is due to the high carbon content and stable structure of long fiber plants. Fig. 6k shows the cross section of the coconut shell fiber. It is hollow cavities with diameter ranging from 5 to 10 μm. The wall of algae become thinner [121]. After chemical activation, the SEM images of four samples are depicted in Fig. 6m–p. From Fig. 6m, the vacancies in cotton stalk are more visible [120]. The biochar of saussurea involucrata stalk shows a distinct hierarchical porous carbon structure. In Fig. 6o, it can be seen that the coconut shell also retains the original long fiber structure. The small particles on the coconut shell are disappeared and leaved holes with a diameter of about 8 μm. This is because KOH corrodes the silicates at high temperatures. Fig. 6p shows that the algae after activated by KOH is flaky and porous [121].

The structural analysis above shows that long fiber plants can maintain the original structural framework after the KOH activation. This special structure accelerates electrolyte ions to transport at active electrode surface, resulting excellent electrochemical performance. Cotton stalk-based active carbon shows electrochemical capacitance of 254 F g^{-1} at current density of 0.2 A g^{-1}. Hierarchical porous saussure involucrata stalk–based carbon possesses a superior specific capacitance of 322 F g^{-1} at a current density of 0.2 A g^{-1}. Active carbon derived from coconut shell displays a electrochemical capacitance of 157 F g^{-1} at a current density of 0.2 A g^{-1}. Because of well-developed transmission channel, it shows an excellent cycling life of 100% specific capacitance retention over 10000 cycles at a current density of 1 A g^{-1}. That hierarchical and flaky structure of algae-based carbon is beneficial for ions diffusion and charge storage. So it shows electrochemical capacitance of 283 F g^{-1} at a current density of 0.2 A g^{-1}. All results above indicate the long fiber biomass have advantages in the synthesis of active materials for energy conversion application.

It is easy to discover that the frameworks of the long fiber-based carbons are clearly associated to the intrinsic one of the raw material. For example, the porous layer active carbon based on cotton stalk

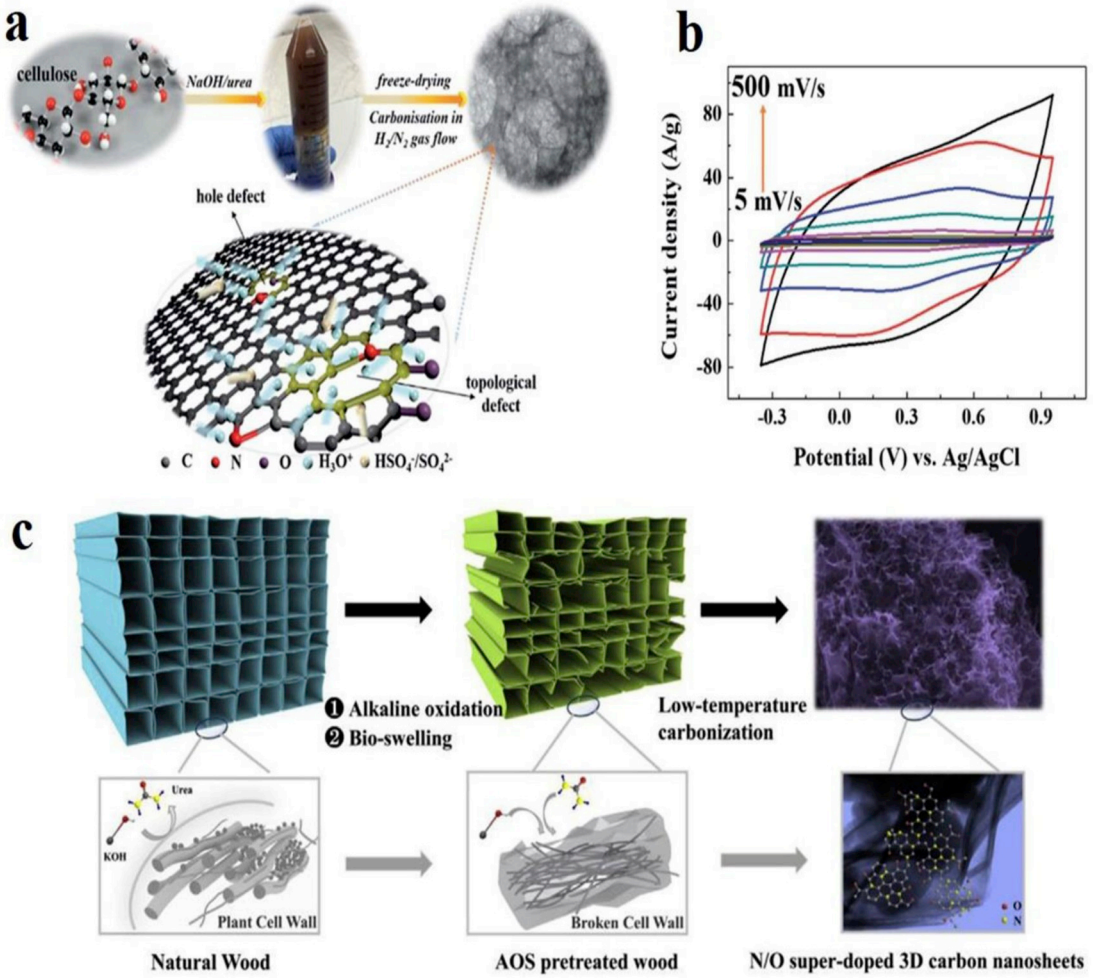

Fig. 7. (a) A schemetic of the preparation process of microcrystalline cellulose-derived porous carbon. (b) CV curves at scan rates 5–500 mV s^{-1} of the as-prepared sample. Reprinted with permission from Ref. [168], Copyright 2019, Royal Society of Chemistry. (c) Schematic illustration of sustainable synthesis and assembly of O/N co-doped 3D carbon nanosheet. Reprinted with permission from Ref. [169], Copyright 2019, Elsevier.

exhibited similar morphology trait to the original one of cotton stalk, which composed of relatively ordered flute pores on the surface, as shown in Fig. 6e and 6m [120]. The hierarchical porous carbon based on coconut shell also indicates similar long fiber-like texture to coconut shell, as shown in Fig. 6g and 6o. The algae based active carbon shows similar hierarchical porous texture to the algae, which further generate a number of cross-linked meso/microporous frameworks after activation, as shown in Fig. 6h and 6p. The cross-linked meso/microporous frameworks offer good electrochemical performance. Mesoporous carbon materials commonly possess wormhole morphology with cylindrical surface. By supposing that the mesopores are cylindrical, electrolyte ions transport through pores to develop electric double-cylinder capacitors. The double cylinder capacitance is calculated by Eqn. (1) [160]:

$$C/S = \frac{\varepsilon_r \varepsilon_0}{b ln(\frac{b}{b-d})} \quad (1)$$

where C is the capacitance, S is the surface area of the cylinder, ε_r is the dielectric constants of the electrolyte and ε_0 is permittivity of the vacuum. b is radius of the outer cylinder, and d is separation distance of the outside and inside cylinders. With regard to micropores, the electrolyte ions will form an electric wire-in-cylinder capacitor (EWCC) because of the very small pore size. The capacitance of the EWCC can be calculated by eqn. (2):

$$C/S = \frac{\varepsilon_r \varepsilon_0}{b_0 ln(\frac{b_0}{a_0})} \quad (2)$$

which b_0 represents radius of the micropore, a_0 represents real size for the electrolyte ions. That radius of the micropore may as well similar to the real size for the electrolyte ions so that achieve better electrochemical performance [161]. The transport behavior of electrolyte ions during charging and discharge process is importantly depend on pore size, pore distribution and curvature [162]. The ion diffusion time (t) is evaluated through relational expression $t = r^2/d$, which r represents ion diffusion length and d represents ion diffusion factor. Active electrode materials within hierarchically pores in 0D, 1D, 2D and 3D endows electrolyte ions in electrode decrease short diffusion distances, so minimizing the diffusion time.

3.2. Graphitization degree

Graphitization degree is also crucial with respect to electrochemical performances of biomass-based carbon materials, such as internal resistance, rate capability, power delivery, and energy efficiency. Improving the graphitization of active carbon promote surface hydrophily for the electrode in aqueous electrolyte, which can accelerate electrolyte ion diffusion as well as charge transport, so benefiting for the supercapacitor performance [91]. As we known, a high electrical conductivity is usually associated with a high graphitization degree. However, it will result in a small specific surface area (SSA) and an undeveloped pore structure. Therefore, there is a compromise between the graphitization degree and pore structure in order to maximize the electrochemical performance. Thermally pyrolysis can increase the graphitization but it consumes much more energy. In addition, it can also reduce accessible surface area as well as pore volume for the active electrode materials. Catalytic graphitization using transition metal is an efficient route to prepare active carbons with a certain graphitization degree. Considering proper activation and catalytic graphitization into consideration can perfectively fabricate hierarchical carbons with high accessible surface area so that outstanding electrochemical performance. Sun et al. synthesized porous 2D nanosheets with a high accessible surface area by a chemical activation and catalytic graphitization method employing coconut shell as raw material [91]. $FeCl_3$ and $ZnCl_2$, acting as a graphitic catalyst and activating reagent respectively, were incorporated with the texture of the coconut shell via adjusting salt ions mass and the heteroatoms type on the coconut shell, so making simultaneous activation as well as graphitization. The obtained 2D nanosheets had excellent electrical conductivity because of a high graphitization degree, accessible surface area of 1874 $m^2 g^{-1}$ and total pore volume of 1.21 $cm^3 g^{-1}$. Without mixing conductive agents, it demonstrated a high capacitance of 268 F g^{-1} at 1 A g^{-1} in KOH electrolyte. What's more, it also exhibited a capacitance of 196 F g^{-1} at 1 A g^{-1} in an organic electrolyte. An energy density of 54.7 Wh kg^{-1} was achieved at a power density of 10 kW kg^{-1}. Zhang et al. synthesized hierarchically active carbon microtubes through the chemical activation and graphitization method using $K_4Fe(CN)_6$, thus offering high conductivity and short ion diffusion route [77]. As-prepared graphitic carbon microtubes also act as a considerable support for loading manganese dioxide. The hybrid electrode showed good electrochemical behaviors, for instance a quite increased specific capacitance (550.8 F g^{-1} at a current density of 2 A g^{-1}), a high capacitance retention of 62% at a high current density of 50 A g^{-1}, and long cycle life of 90% capacitance retention after 5000 cycles. Jiang and co-workers reported a facile method to synthesize catalyst-free, flexible, and highly graphitized carbon aerogels based on bacterial cellulose [163]. Because of their unique nanostructure and large mesopore proportion, the carbon materials exhibit an area capacitance of 62.2 mF cm^2, which is higher than most of the reported values in the literature. Owing to the excellent conductivity, the highly graphitized carbon aerogels can facilitate electron transport, and they show excellent electrochemical capacitances in 6 M KOH electrolyte.

4. Surface properties

Exactly as the specific surface area and pores distribution, the surface information of biomass-based active electrode materials act a significant factor on the supercapacitor performance. Whereas the pore frameworks of active materials can be adjusted through appropriate option of activation method and process that make fabrication of activated carbon with different percent of micro, meso and macropores in various dimensions; the variety and content of surface functional group could be optimized via proper thermal and chemical post-treatments. Adjustment of surface functional groups for carbon commonly bring about changes in the physical and chemical properties such as wettability, electrical conductivity, capacitance of the biomass-based carbon material.

Recent study proved that the functional groups or doped elements like nitrogen (N), oxygen (O), phosphorus (P), Sulphur (S), boron (B), can significantly increase available surface properties like wettability, electrical resistance or adding pseudocapacitance of the carbon electrodes. A number of researchers synthesized heteroatom doped biomass-based active material via blending raw source with some heteroatom-rich precursors and a series of activation method.

O incorporating into carbon structure is beneficial for improving the wettability, widening working voltage window and increasing energy density of supercapacitors in aqueous electrolytes. In general, O-doping is achieved through pyrolysis of O-containing biomass source or KOH chemical activation [164]. Zhang and cooperators synthesized a O-containing carbon materials with stacked layer texture employing gelatin as the source [165]. The as-prepared O-containing carbon demonstrated electrochemical capacitance of 276.6 F g^{-1} at a current density of 1 A g^{-1} in a two-electrode system and still retained 72.3% of capacitance retention at 100 A g^{-1}. Large proportion of O (16.22 wt%) can improve pseudocapacitance and rate performance.

N is another extensive researched heteroatom during the preparation for active electrode materials. It is believed that doping N can increase conductivity of carbon materials so that add pseudocapacitance, resulting into a significant increase in the capacitance. In the carbon materials, N element usually is categorized into 3 varieties: pyridinic-type nitrogen, pyrrolic-type nitrogen and quaternary-type nitrogen, pyridinic-type N and pyrrolic-type N, are believed to play pseudocapacitance role, while quaternary-type N can improve charge transfer through the carbon electrode. Generally, N functional groups are doped

into active carbon structure via simple pyrolysis of N-rich carbon precursors or adding N-containing source. Hou et al. developed N-containing hierarchical ultrathin carbon layers through activation and graphitization process employing raw silk. The as prepared active electrode material showed excellent property in SCs [166]. Zhou and cooperators synthesized special N-rich well-organized mesoporous carbon, which has a large accessible surface area of 1030 $m^2 g^{-1}$, same size of mesopores about 15.0 nm diameters and a large nitrogen percentage of 7 wt%. These special structural features ensure active material a good capacitance of 264 F g^{-1} in supercapacitors [167]. Lu et al. prepared porous carbon materials with intrinsic defects and nitrogen doping using microcrystalline cellulose as the precursor (Fig. 7a and b) [168]. Because the continuous hierarchical porous structure and high N content can more fully utilize for charge storage via electrical double-layer and pseudocapacitive mechanisms, respectively, the obtained materials displayed an exceptional specific capacitance of 426 F g^{-1}, an excellent rate capability and superior cycling stability. Currently, Liu et al. fabricated a mass of three dimensional O/N co-doped carbon nanosheet from woody precursor via sequential alkaline oxidation, bio-swelling and low-temperature carbonization. (Fig. 7c) [169]. During the micromorphological regulation, KOH solution hydrolyse hemicellulose, while H_2O_2 continuously oxidizes lignin. Urea is used N precursor in order to incorporated N in resulted material. The doped carbon nanosheets deliver an impressive superior capacitance of 508 F g^{-1} at 1 A g^{-1} and long lifetime over 12 thousand cycles with 95% capacitance retention.

Similar to N-doping, other heteroatoms like P, S and B, can also improve the electrical conductivity, enhance the effective specific surface area and add pseudocapacitance, making carbon with a good electrochemical performance. Currently, Qiu et al. fabricated a mass of flexible B/N co-doped carbon via hard template and subsequent annealing method [119]. Boric acid is used template as well as boron precursor in order to incorporate B in resulted material. The doped carbon nanosheets deliver an impressive superior capacitance of 268 F g^{-1} at 0.1 A g^{-1} and long lifetime over 15 thousand cycles with 110% capacitance retention. Another example for N, B containing hierarchically porous carbon nanotube is obtained using dandelion fluff [82]. The bundled and porous framework leads to quick charge transfer and ion diffusion. Thanks to N and B heteroatoms doping, the electrode demonstrates very stable framework, long cycle life and an outstanding energy density of 12.2 Wh L^{-1} at the power density of 699.8 W L^{-1}. Huang et al. fabricated P-containging porous carbon via H_3PO_4 chemical activation of discarded coffee grounds [170]. The resulted active material displayed superior specific capacitances using 6 M KOH as electrolytes. It was observed that prepared supercapacitors could operate at a high working voltage due to P-containing groups on the carbon surface. A superior energy density of 15 W h kg^{-1} can be reached at a power density of 75 W kg^{-1}. Xu et al. fabricated S and N co-doped hierarchically porous active carbon employing broad bean shells rich in amino acids and vitamins as raw material [171].

Broad bean was high temperature pyrolyzed at 800 °C for 2 h and subsequently activated by chemical reagent at high temperature for 1 h with N_2 gas atmosphere with a heating rate of 3 °C min^{-1}. The incorporated S element enhanced space utilization through unique electrosorption of electroactive ions. That doped N elevated both the electrical conductivity and the wettability of the electrode. Furthermore, elements S and N containing functional groups introduced the pseudocapacitance. So obtained carbon material displayed a specific capacitance of 202 F g^{-1} at a current density of 0.5 A g^{-1} in 6 M KOH electrolyte and remained 64% capacitance at 10 A g^{-1} despite the medium specific surface area (655 $m^2 g^{-1}$) of the carbon.

These heteroatoms are either derived from the precursor and form part of the active carbon structure or introduced by an effective activation method. In a word, heteroatoms mixed into carbon have been verified to be efficient in enhancing the electrochemical properties of carbon materials.

5. Prediction by machine learning

In the topic of energy conversion, researchers used various methods to adjust the microstructure, surface area as well as porosity of active electrode materials. The macroscopic and microcosmic structure features of electrode materials affect electrochemical performance. However, the widely accepted structure-performance relationship is still unclear. Traditional EDLCs theory and models only give a mathematical equation for EDLCs' surface. There is a big challenge to obtain the relations between the microscopic structures and the macroscopic performances for predicting the capacitance of carbon-based supercapacitors. With the development in computational technology and computer science, the application of machine learning (ML) technology for the material synthesis has become the general trend [172]. ML is a data-based method, which is often treated as a black box, and the outputs are difficult to explain. It provides powerful tools that can take advantage of previously generated data to better understand the relationships between structure of origin materials and properties & performance of EDLCs. To be specific, in the past we could only analyze the function between the structure and performance of materials from a few samples, but now we can analyze this complex relationship from available databases including great numbers of known structure and performance with the help of ML technology. For example, Daniel et al. integrated ML approach to find materials for clean energy, which provides a vision for the next generation of autonomous materials discovery, so decreasing the time to application of novel materials by an order of magnitude [173]. José Darío et al. used a combination of ML driven electronic structure calculations to forecast Flory–Huggins coefficient of new photovoltaics materials [174].

Current research in supercapacitors has obtained much attention on a variety of biomass-based carbon electrode materials. Given the nature structure of various materials, the ML modeled by structure–performance relationship can provide good guideline for electrode materials selection. To predict the EDLCs capacitance, a sequential procedure is used. The first step is to collect the experimental data including the physical and chemical properties of porous carbon electrode materials or the test potential windows. Then, the experimental data are applied to predict the EDLCs capacitance using different ML models such as linear regression (LR), support vector regression (SVR) and artificial neural network (ANN) models [175]. LR has predictors that are linear in the model parameters, which is easy to interpret, and fast in making predictions. However, the limit of LR models is its low predictive accuracy. SVR is a regression technique with excellent performances in regression and time series prediction application, allowing categorising the input data using separating lines or planes. ANN model generally includes input layers, hidden layers and output layers, and each layer consists of nodes connected with a certain weight to all nodes in the next layer. Except for the input nodes, each node is a processing element with a nonlinear activation function such as a sigmoid function that enables the network to compute complex nonlinear problems. ANN utilizes the 'back propagation' technique to train the network, which means to change connection weights while passing through the nodes in order to minimize the error. The training process stops improving, which means that no further decrease occurs in the errors of cross-validation samples. The algorithms of ML models were conducted in the machine learning open source package WEKA. Each method includes its own parameters that must be specified. Specifically, the datasets were evenly split into several folds. Some folds were used for training while the remaining fold was used for testing. The calculation process was repeated using a different fold for testing in each cycle. The performance of each model was given by the average of the accuracies of all the folds. The correlation coefficient (R^2), root mean square error (RMSE) were used to evaluate the accuracies of different ML models in predicting EDLCs capacitance [176].

$$R^2 = 1 - \frac{\sum_{i=1}^{n}(y_i - u_i)^2}{\sum_{i=1}^{n}(y_i - \overline{u})^2} \quad (3)$$

$$\mathrm{RMSE} = \sqrt{\frac{\sum_{i=1}^{n}(y_i - u_i)^2}{n}} \quad (4)$$

where n, y_i, u_i and u are, the number of data points, the value calculated from the ML, the experimental value, and the average of all experimental data.

ANN has been widely employed for energy harvesting and production [177,178]. Farsi et al. used ANN to predict the electrochemical behaviors based on a supercapacitor model. Crystal size, surface lattice length, exchange current density of the active electrode material and the discharge current were inputs, energy density and power density were the outputs. A neural network including two hidden layers (6 nodes and 15 nodes) was discovered to have high power of modeling the electrochemical behaviors with the convergence [179]. Dongale at el. modeled cyclic voltammetery using ANN. Fig. 8a demonstrates the model structure for supercapacitor, which include one input layer, one output layer and one hidden layer. In their programming process, the Levenberg–Marquart back propagation algorithm with the sigmoid nonlinear function was employed to optimize the predicting power of ANNs. The neural model demonstrated the superior behavior with the error rate 1.24%, 1.03%, 0.87%, 1.17%, and 1.28% for samples which electrodeposited different mass of MnO_2 [180]. Weigert predicted the state-of-charge of batteries and battery–supercapacitor hybrid systems. The prediction shows good performance with a correlation coefficient above 0.95 (Fig. 8b) [181]. In 2018, Zhu et al. complied over 10,000 data points for the capacitance of carbon-based supercapacitors from more than 1000 publications. The authors studied the impact of five variables (specific surface area, calculated pore size, I_D/I_G ratio, N-doping level and voltage window) on capacitance by the ANN method. It is demonstrated that the ANN method is more accurate with a higher correlation coefficient ($R^2 = 0.91$) through comparing the ANN method with two different machine learning models (linear regression and Lasso) [182]. The superiority of ANN is attributed its ability in prediction of regression value with multi-factor control. Recently, Ma's group resorted ANN model to predict energy storage for supercapacitors (Fig. 8c–d). A data set comprising 200 biomass-based active carbon was divided into training subset and test subset by cross-validation. As shown in Fig. 8c, the specific capacitance is simulated by many kinds of input features such as aspect ratio ($r_{L/D}$), cellulose ratio (CL (%)), specific surface area (S_{BET}), pore volume (V_{tot}), internal resistance (R_s) and so on. Levenberg–Marquart back propagation algorithm with sigmoid and ReLu non-linear function is applied to train the model. The model yielded accurate predictions of specific capacitance with mean square error to be as low as 4.39. The random forest algorithm was used to calculate the relative contribution of each input (structural features) to the output (specific capacitance). The machine learning used in this paper is able to predict the function between the structure and performance from currently available databases, which include great numbers of known structure of biomass materials. The result indicates the specific surface area, resistance, and total pore volume are the three most important variables, with a weight of 30.1%, 19.4% and 18.7%, respectively. This pointed out promising direction of electrode synthesis [121].

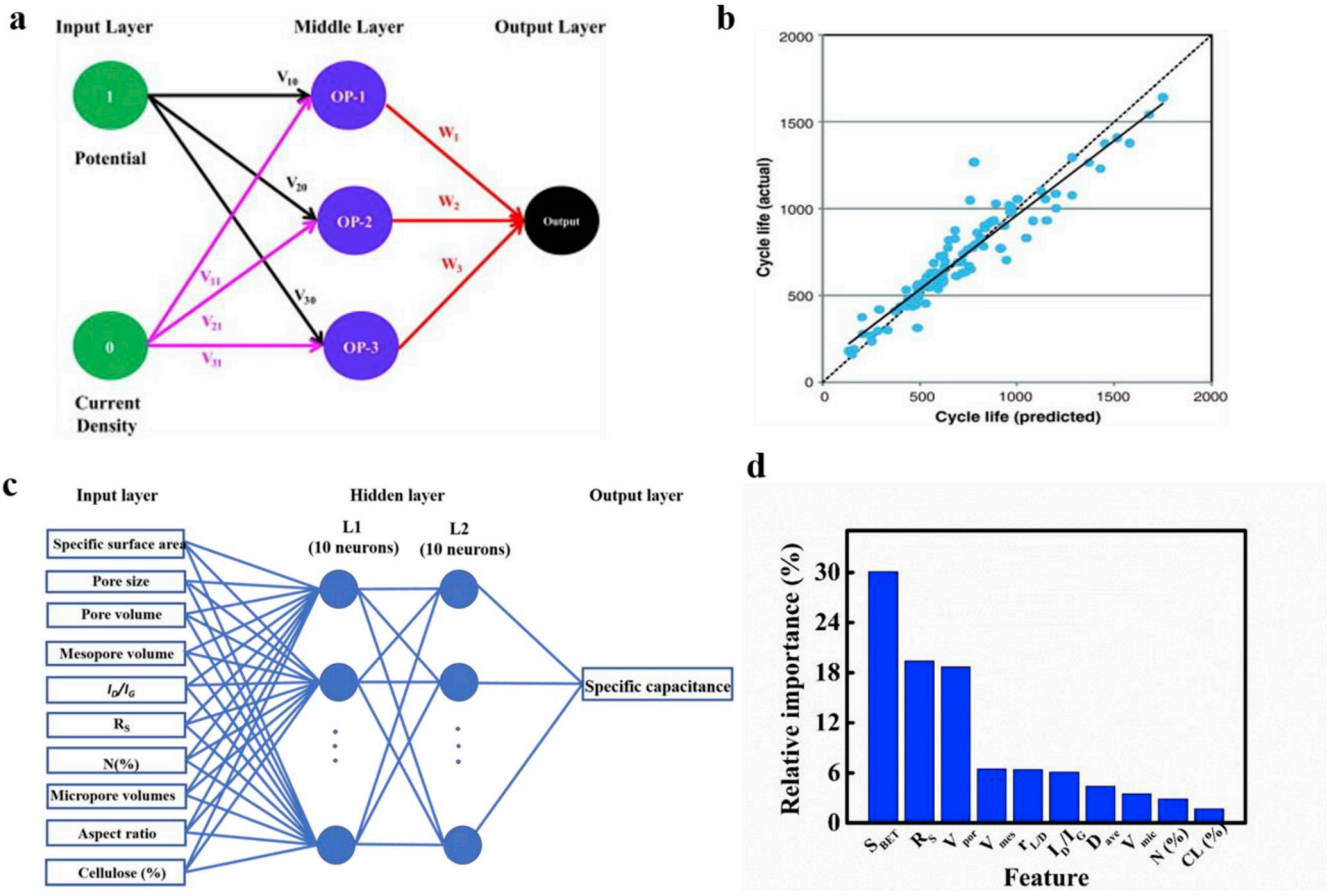

Fig. 8. (a) Multilayer structure of a supercapacitor model. Reprinted with permission from Ref. [180], Copyright 2015, Elsevier. (b) Predicted cycle life at a discharge current of 2.0 A. Reprinted with permission from Ref. [181], Copyright 2011, Elsevier. (c) Artificial neural network model for supercapacitor. (d) The relative importance of inputs to output. Reprinted with permission from Ref. [121], Copyright 2019, Royal Society of Chemistry.

6. Challenges and perspectives

Biomass is one of the most abundant materials on the earth. Therefore, biomass-derived carbon materials have become an effective solution toward coping with severe environmental issues and energy crises. Biomass based carbon materials with good electrochemical performance have been fabricated via various methods. However, it is still confronted with several challenges. For example, biomass generally has irregular morphologies, so that pore properties like shape and structure are difficult to tune precisely, which limits the rate performance and power density. What's more, the effects of pore size, surface area and surface chemistry on the electrochemical performance of biomass-derived energy storage devices are unknown to a large extent. It is still a big challenge for us to investigate the diffusion process of ions in hierarchical pore structure. To address the aforementioned issues, some important research directions in the area of material synthesis and structural design for supercapacitor electrodes are proposed as follows. (1) Considering the diversity of biomass resources, fundamental studies are necessary to understand and control the properties of biomass derived carbon materials that are prepared using different biomass precursors and methods. In situ technologies, such as X-ray absorption, X-ray diffraction and nuclear magnetic resonance, may be powerful tools for understanding these fundamental issues. (2) Giving deep insight into machine learning (ML) for energy storage applications. In this regard, developing proper theoretical models is beneficial to predict the capacitive properties of biomass precursor and active carbon materials, which might be acted as a sophisticated criterion for selecting precursor with optimized performance. (3) More researches should be carried out in the relationship between heteroatom rich in the biomass and proprieties of supercapacitors. It is an effective way as it can adjust the surface morphology as well as provide extra functions. Recently, our group use coconut silk enriched heteroatoms to prepare composite carbon. Heteroatom (N, S, SiO_2) in coconut silk may be beneficial to pore-forming, which shortens the ion/charge transportation distance (not published). Last but not least, with regard to some specific applications such as flexible and miniaturized devices [183,184], a flexible electrode having the desired mechanical and electrochemical properties is demanded. Biomass offers opportunities for making flexible electrodes. This will open up a new research area. With continual research on this research topic, there could be great opportunities to achieve practical applications of biochar materials in the fields of renewable energy conversion and storage.

7. Summary

In summary, the applications of plentiful biomass in fabricate biomass-based materials with excellent electrochemical behaviors for supercapacitor is sustainable and low cost. The electrochemical performance is strongly dependent on the chemical composition, pore structure of the biomass source and experimental conditions. Therefore, it needs proper design in the selection of source material, appropriate pyrolysis or activation method so as to attain well-quality biomass-based product. Considering the diversity of biomass resources, this review is completed a detailed research on the electrocapacitive properties from biomass species and organs. It is a good practice to analyze precursor in term of plant, microorganism and animal remains, and summarized different promising features specially so as to optimize the of electrochemical property of biomass-based active carbon. They are different from structure and compositional design, such as preparing 0D-3D interconnected porous frameworks; heteroatom doping and graphitization degree, which can enhance the energy density and power density. The successful transformation from biomass to nanostructure carbon develops a novel route to use naturally available frameworks. In spite of the advanced study about the biomass-based material for supercapacitors has demonstrated comparably high electrochemical performance, high-rate capability and cycling ability, a number of critical challenges and prospects are pointed out in the progress of biomass-based carbon in supercapacitors at end of this review. This review can provide a general guideline for the preparation of next-generation energy storage devices.

Declaration of competing interest

The co-authors declare that they have no known competing financial interests or personal relationships that could have appeared to influence the work reported in this paper.

Acknowledgements

This work was financially supported by the National Natural Science Foundation of China (No. 11774255) and the Key Project of Natural Science Foundation of Tianjin City, China (No. 17JCZDJ30100).

References

[1] Y. Zhang, X. Liu, S. Wang, L. Li, S. Dou, Adv. Energy Mater. 7 (21) (2017) 1700592.
[2] S. Hatfield-Dodds, H. Schandl, D. Newth, M. Obersteiner, Y. Cai, T. Baynes, J. West, P. Havlik, J. Clean. Prod. 144 (2017) 403–414.
[3] X. Chen, C. Li, M. Gratzel, R. Kostecki, S. Mao, Chem. Soc. Rev. 41 (23) (2012) 7909–7937.
[4] S. Chu, A. Majumdar, Nature 488 (7411) (2012) 294–303.
[5] H. Wang, Y. Yang, L. Guo, Adv. Energy Mater. 7 (23) (2017), 1700663.
[6] Z. Yu, L. Tetard, L. Zhai, J. Thomas, Energy Environ. Sci. 8 (3) (2015) 702–730.
[7] Z. Wang, D. Shen, C. Wu, S. Gu, Green Chem. 20 (22) (2018) 5031–5057.
[8] J. Jiang, Y. Zhang, P. Nie, G. Xu, M. Shi, J. Wang, Y. Wu, R. Fu, H. Dou, X. Zhang, Adv. Sustainable Syst. 2 (1) (2018), 1700110.
[9] Q. Wang, J. Yan, Z. Fan, Energy Environ. Sci. 9 (3) (2016) 729–762.
[10] Y. Bai, B. Shen, S. Zhang, Z. Zhu, S. Sun, J. Gao, B. Li, Y. Wang, R. Zhang, F. Wei, Adv. Mater. 31 (9) (2018), 1800680.
[11] V. Strauss, K. Marsh, M.D. Kowal, M. El-Kady, R.B. Kaner, Adv. Mater. 30 (8) (2018), 1704449.
[12] K.S. Kim, Y. Zhao, H. Jang, S.Y. Lee, J.M. Kim, K.S. Kim, J.H. Ahn, P. Kim, J. Y. Choi, B.H. Hong, Nature 457 (7230) (2009) 706–710.
[13] F. Abnisa, W.M.A.W. Daud, Energy Convers. Manag. 87 (2014) 71–85.
[14] S. Gillet, M. Aguedo, L. Petitjean, A.R.C. Morais, A.M. da Costa Lopes, R. M. Łukasikd, P.T. Anastas, Green Chem. 19 (18) (2017) 4200–4233.
[15] Q. Niu, K. Gao, Q. Tang, L. Wang, L. Han, Carbon 123 (2017) 290–298.
[16] S. Zhou, L. Zhou, Y. Zhang, J. Sun, J. Wen, Y. Yuan, J. Mater. Chem. 7 (9) (2019) 4217–4229.
[17] J. Wang, P. Nie, B. Ding, S. Dong, X. Hao, H. Dou, X. Zhang, J. Mater. Chem. 5 (6) (2017) 2411–2428.
[18] L. Jiang, L. Sheng, Z. Fan, Sci. China Mater. 61 (2) (2018) 133–158.
[19] Z. Bi, Q. Kong, Y. Cao, G. Sun, F. Su, X. Wei, X. Li, A. Ahmad, L. Xie, C. Chen, J. Mater. Chem. 7 (27) (2019) 16028–16045.
[20] H. Yang, S. Ye, J. Zhou, T. Liang, Frontiers. Chem. 7 (2019) 274.
[21] H. Lu, X. Zhao, Sustain. Energy. Fuels. 1 (6) (2017) 1265–1281.
[22] S.E.M. Pourhosseini, O. Norouzi, P. Salimi, H.R. Naderi, ACS Sustain. Chem. Eng. 6 (4) (2018) 4746–4758.
[23] S. Gao, X. Li, L. Li, X. Wei, Nano Energy 33 (2017) 334–342.
[24] Y. Zhong, X. Xia, S. Deng, J. Zhan, R. Fang, Y. Xia, X. Wang, Q. Zhang, J. Tu, Adv. Energy Mater. 8 (1) (2018), 1701110.
[25] C.K. Ranaweera, P.K. Kahol, M. Ghimire, S.R. Mishra, K.G. Ram, J. Carbon Res. 3 (3) (2017) 25.
[26] K. Zou, Y. Deng, J. Chen, Y. Qian, Y. Yang, Y. Li, G. Chen, J. Power Sources 378 (2018) 579–588.
[27] C. Lu, Y. Huang, Y. Wu, J. Li, J. Cheng, J. Power Sources 394 (2018) 9–16.
[28] Q. Tian, X. Wang, X. Xu, M. Zhang, L. Wang, X. Zhao, Z. An, H. Yao, J. Gao, Mater. Chem. Phys. 213 (2018) 267–276.
[29] J. Xia, N. Zhang, S. Chong, D. Li, Y. Chen, C. Sun, Green Chem. 20 (3) (2018) 694–700.
[30] X. Wang, S. Yun, W. Fang, C. Zhang, X. Liang, Z. Lei, Z. Liu, ACS Sustain. Chem. Eng. 6 (9) (2018) 11397–11407.
[31] T. Ramesh, N. Rajalakshmi, K.S. Dhathathreyan, L.R.G. Reddy, ACS Omega 3 (10) (2018) 12832–12840.
[32] F. Zeng, Z. Li, X. Li, J. Wang, Z. Kong, Y. Sun, Z. Liu, H. Feng, Appl. Surf. Sci. 467 (2019) 229–235.
[33] Y. Liu, B. Huang, X. Lin, Z. Xie, J. Mater. Chem. 5 (25) (2017) 13009–13018.
[34] Z. Wang, H. Guo, F. Shen, G. Yang, Y. Zhang, Y. Zeng, L. Wang, H. Xiao, S. Deng, Chemosphere 119 (2015) 646–653.
[35] D. Kang, Q. Liu, J. Gu, Y. Su, W. Zhang, D. Zhang, ACS Nano 9 (11) (2015) 11225–11233.
[36] X. Zheng, J. Luo, W. Lv, D.W. Wang, Q.H. Yang, Adv. Mater. 27 (36) (2015) 5388–5395.
[37] N. Yoshizawa, K. Maruyama, Y. Yamada, M. Zielinska-Blajat, Fuel 79 (2000) 1461–1466.

[38] K.R. Thines, E.C. Abdullah, N.M. Mubarak, M. Ruthiraan, Renew. Sustain. Energy Rev. 67 (2017) 257–276.
[39] B. Duan, X. Gao, X. Yao, Y. Fang, L. Huang, J. Zhou, L. Zhang, Nano Energy 27 (2016) 482–491.
[40] R. Wang, P. Wang, X. Yan, J. Lang, C. Peng, Q. Xue, ACS Appl. Mater. Interfaces 4 (11) (2012) 5800–5806.
[41] S. Laurichesse, L. Avérous, Prog. Polym. Sci. 39 (7) (2014) 1266–1290.
[42] M.-A. ArsÂne, K. Bilba, H. Savastano Junior, K. Ghavami, Mater. Res. 16 (4) (2013) 903–923.
[43] A.R. Reed, P.T. Williams, Int. J. Energy Res. 28 (2) (2004) 131–145.
[44] R. Biswas, H. Uellendahl, B.K. Ahring, BioEnergy Res 8 (3) (2015) 1101–1116.
[45] G. Zu, J. Shen, L. Zou, F. Wang, X. Wang, Y. Zhang, X. Yao, Carbon 99 (2016) 203–211.
[46] D. Shan, J. Yang, W. Liu, J. Yan, Z. Fan, J. Mater. Chem. 4 (35) (2016) 13589–13602.
[47] L. Wei, M. Sevilla, A.B. Fuertes, R. Mokaya, G. Yushin, Adv. Energy Mater. 1 (3) (2011) 356–361.
[48] X. Tian, S. Zhu, J. Peng, Y. Zuo, G. Wang, X. Guo, N. Zhao, Y. Ma, L. Ma, Electrochim. Acta 241 (2017) 170–178.
[49] J. Tian, Z. Liu, Z. Li, W. Wang, H. Zhang, RSC Adv. 7 (20) (2017) 12089–12097.
[50] W.-J. Liu, H. Jiang, H.-Q. Yu, Green Chem. 17 (11) (2015) 4888–4907.
[51] W. Zhang, H. Lin, Z. Lin, J. Yin, H. Lu, D. Liu, M. Zhao, ChemSusChem 8 (12) (2015) 2114–2122.
[52] H. Peng, N. Wang, Z. Hu, Z. Yu, Y. Liu, J. Zhang, R. Ruan, Ind. Crop. Prod. 37 (1) (2012) 41–50.
[53] Y. Wang, R. Yang, M. Li, Z. Zhao, Ind. Crop. Prod. 65 (2015) 216–226.
[54] Y. Cai, Y. Luo, H. Dong, X. Zhao, Y. Xiao, Y. Liang, H. Hu, Y. Liu, M. Zheng, J. Power Sources 353 (2017) 260–269.
[55] H. Jin, J. Hu, S. Wu, X. Wang, H. Zhang, H. Xu, K. Lian, J. Power Sources 384 (2018) 270–277.
[56] N. Sudhan, K. Subramani, M. Karnan, N. Ilayaraja, M. Sathish, Energy Fuels 31 (1) (2016) 977–985.
[57] H. Yu, W. Zhang, T. Li, L. Zhi, L. Dang, Z. Liu, Z. Lei, RSC Adv. 7 (2) (2017) 1067–1074.
[58] A. Gopalakrishnan, C. Kong, S. Badhulika, New J. Chem. 43 (3) (2019) 1186–1194.
[59] C. Wang, D. Wu, H. Wang, Z. Gao, F. Xu, K. Jiang, J. Mater. Chem. 6 (3) (2018) 1244–1254.
[60] W. Liu, J. Mei, G. Liu, Q. Kou, T. Yi, S. Xiao, ACS Sustain. Chem. Eng. 6 (2018) 11595–11605.
[61] X. Zhu, S. Yu, K. Xu, Y. Zhang, L. Zhang, G. Lou, Y. Wu, E. Zhu, H. Chen, Z. Shen, B. Bao, S. Fu, Chem. Eng. Sci. 181 (2018) 36–45.
[62] Q. Wang, Y. Zhang, J. Xiao, H. Jiang, T. Hu, C. Meng, J. Alloys Compd. 782 (2019) 1103–1113.
[63] K. Wu, B. Gao, J. Su, X. Peng, X. Zhang, J. Fu, S. Peng, P.K. Chu, RSC Adv. 6 (36) (2016) 29996–30003.
[64] X. Wei, H. Zou, S. Gao, J. Mater. Chem. 5 (1) (2017) 181–188.
[65] E. Hao, W. Liu, S. Liu, Y. Zhang, H. Wang, S. Chen, F. Cheng, S. Zhao, H. Yang, J. Mater. Chem. 5 (5) (2017) 2204–2214.
[66] L. Zheng, S. Wang, Y. Yang, X. Fu, T. Jiang, J. Yang, ACS Omega 4 (3) (2019) 5904–5914.
[67] G. Zhu, L. Ma, H. Lv, Y. Hu, T. Chen, R. Chen, J. Liang, X. Wang, Y. Wang, C. Yan, Z. Tie, Z. Jin, J. Liu, Nanoscale 9 (3) (2017) 1237–1243.
[68] S. Qu, J. Wan, C. Dai, T. Jin, F. Ma, J. Alloys Compd. 751 (2018) 107–116.
[69] J. Huang, L. Chen, H. Dong, Y. Zeng, H. Hu, M. Zheng, Y. Liu, Y. Xiao, Y. Liang, Electrochim. Acta 258 (2017) 504–511.
[70] D. He, W. Zhao, P. Li, S. Sun, Q. Tan, K. Han, L. Liu, L. Liu, X. Qu, J. Alloys Compd. 773 (2019) 11–20.
[71] X. Yang, C. Li, Y. Chen, J. Phys. D Appl. Phys. 50 (5) (2017), 055501.
[72] J. Chang, Z. Gao, X. Wang, D. Wu, F. Xu, X. Wang, Y. Guo, K. Jiang, Electrochim. Acta 157 (2015) 290–298.
[73] T. Wei, X. Wei, L. Yang, H. Xiao, Y. Gao, H. Li, J. Power Sources 331 (2016) 373–381.
[74] R.P. Panmand, P. Patil, Y. Sethi, S.R. Kadam, M.V. Kulkarni, S.W. Gosavi, N. R. Munirathnama, B.B. Kale, Nanoscale 9 (14) (2017) 4801–4809.
[75] D. Yu, C. Chen, G. Zhao, L. Sun, B. Du, H. Zhang, Z. Li, Y. Sun, F. Besenbacher, M. Yu, ChemSusChem 11 (10) (2018) 1678–1685.
[76] K. Wang, R. Yan, N. Zhao, X. Tian, X. Li, S. Lei, Y. Song, Q. Guo, L. Liu, Mater. Lett. 174 (2016) 249–252.
[77] X. Zhang, K. Zhang, H. Li, Q. Cao, L. Jin, P. Li, J. Power Sources 344 (2017) 176–184.
[78] X.-L. Su, M.-Y. Cheng, L. Fu, J.-H. Yang, X.-C. Zheng, X.-X. Guan, J. Power Sources 362 (2017) 27–38.
[79] Y. Li, G. Wang, T. Wei, Z. Fan, P. Yan, Nano Energy 19 (2016) 165–175.
[80] L. Xie, G. Sun, F. Su, X. Guo, Q. Kong, X. Li, X. Huang, L. Wan, W. Song, K. Li, C. Lv, C. Chen, J. Mater. Chem. 4 (5) (2016) 1637–1646.
[81] Y. Wei, Chem. Lett. 43 (2) (2014) 216–218.
[82] J. Zhao, Y. Li, G. Wang, T. Wei, Z. Liu, K. Cheng, K. Ye, K. Zhu, D. Cao, Z. Fan, J. Mater. Chem. 5 (44) (2017) 23085–23093.
[83] D.R. Feumba, R.P. Ashwini, European J. Food Sci Techn. 4 (2016) 12–21.
[84] Y. Lin, Z. Chen, C. Yu, W. Zhong, ACS Sustain. Chem. Eng. 7 (3) (2019) 3389–3403.
[85] X. Dong, H. Jin, R. Wang, J. Zhang, X. Feng, C. Yan, S. Chen, S. Wang, J. Wang, J. Lu, Adv. Energy Mater. 8 (11) (2018), 1702695.
[86] E. Ciftyurek, D. Bragg, O. Oginni, R. Levelle, K. Singh, Environ. Prog. Sustain. Energy 38 (3) (2019).
[87] H. Fu, Z. Xu, R. Li, W. Guan, K. Yao, J. Huang, J. Yang, X. Shen, ACS Sustain. Chem. Eng. 6 (2018) 14751–14758.
[88] M. Song, Y. Zhou, X. Ren, J. Wan, Y. Du, G. Wu, F. Ma, J. Colloid Interface Sci. 535 (2019) 276–286.
[89] A.A. Mohammed, C. Chen, Z. Zhu, J. Power Sources 417 (2019) 1–13.
[90] A. Jain, C. Xu, S. Jayaraman, R. Balasubramanian, J.Y. Lee, M.P. Srinivasan, Microporous Mesoporous Mater. 218 (2015) 55–61.
[91] L. Sun, C. Tian, M. Li, X. Meng, L. Wang, R. Wang, J. Yin, H. Fu, J. Mater. Chem. 1 (21) (2013) 6462–6470.
[92] X. Qiu, L. Wang, H. Zhu, Y. Guan, Q. Zhang, Nanoscale 9 (22) (2017) 7408–7418.
[93] J. Xu, Q. Gao, Y. Zhang, Y. Tan, W. Tian, L. Zhu, L. Jiang, Sci. Rep. 4 (2014) 5545.
[94] G. Yang, S. Park, J. Alloys Compd. 741 (2018) 360–367.
[95] F. Sun, L. Wang, Y. Peng, J. Gao, X. Pi, Z. Qu, G. Zhao, Y. Qin, Appl. Surf. Sci. 436 (2018) 486–494.
[96] Z. Xiao, W. Chen, K. Liu, P. Cui, D. Zhan, Int. J. Electrochem. Sci. 13 (2018) 5370–5381.
[97] Q. Zhang, K. Han, S. Li, M. Li, J. Li, K. Ren, Nanoscale 10 (5) (2018) 2427–2437.
[98] L. Hu, Q. Zhu, Q. Wu, D. Li, Z. An, B. Xu, ACS Sustain. Chem. Eng. 6 (11) (2018) 13949–13959.
[99] J. Liu, H. Li, H. Zhang, Q. Liu, R. Li, B. Li, J. Wang, J. Solid State Electrochem. 257 (2017) 64–71.
[100] Y.H. Jung, T.H. Chang, H. Zhang, C. Yao, Q. Zheng, V.W. Yang, H. Mi, M. Kim, S. J. Cho, D.W. Park, H. Jiang, J. Lee, Y. Qiu, W. Zhou, Z. Cai, S. Gong, Z. Ma, Nat. Commun. 6 (2015) 7170.
[101] G. Liu, H. Wang, B. Zhou, X. Guo, X. Hu, J. Med. Plants Res. 4 (12) (2010) 1222–1227.
[102] J. Arroyo, V. Farkas, A.B. Sanz, E. Cabib, Cell Microbiol. 18 (9) (2016) 1239–1250.
[103] C. Long, X. Chen, L. Jiang, L. Zhi, Z. Fan, Nano Energy 12 (2015) 141–151.
[104] P. Yadav, A. Basu, A. Suryawanshi, O. Game, S. Ogale, Adv. Mater. Interfaces 3 (2016), 1600057.
[105] D. Chen, L. Li, Y. Xi, J. Li, M. Lu, J. Cao, W. Han, Electrochim. Acta 286 (2018) 264–270.
[106] N. Guo, M. Li, Y. Wang, X. Sun, F. Wang, R. Yang, ACS Appl. Mater. Interfaces 8 (49) (2016) 33626–33634.
[107] Q. Yao, H. Wang, C. Wang, C. Jin, Q. Sun, ACS Sustain. Chem. Eng. 6 (4) (2018) 4695–4704.
[108] D. Wang, Z. Xu, Y. Lian, C. Ban, H. Zhang, J. Colloid Interface Sci. 542 (2019) 400–409.
[109] M. Fu, W. Chen, J. Ding, X. Zhu, Q. Liu, J. Alloys Compd. 782 (2019) 952–960.
[110] Z. Xu, Y. Li, D. Li, D. Wang, J. Zhao, Z. Wang, M.N. Banis, Y. Hu, H. Zhang, Appl. Surf. Sci. 444 (2018) 661–671.
[111] S. Lei, L. Chen, W. Zhou, P. Deng, Y. Liu, L. Fei, W. Lu, Y. Xiao, B. Cheng, J. Power Sources 379 (2018) 74–83.
[112] J. Niu, R. Shao, J. Liang, M. Dou, Z. Li, Y. Huang, F. Wang, Nano Energy 36 (2017) 322–330.
[113] L. Tang, Y. Zhou, X. Zhou, Y. Chai, Q. Zheng, D. Lin, J. Mater. Sci. 10 (2018) 1–10.
[114] H. Xu, C. Wu, X. Wei, S. Gao, J. Mater. Chem. 5 (31) (2018) 15340–15347.
[115] M. Liu, J. Niu, Z. Zhang, M. Dou, F. Wang, Nano Energy 51 (2018) 366–372.
[116] Y. Zhou, J. Ren, Y. Yang, Q. Zheng, J. Liao, F. Xie, W. Jie, D. Lin, J. Solid State Chem. 268 (2018) 149–158.
[117] A. Mondal, K. Kretschmer, Y. Zhao, H. Liu, H. Fan, G. Wang, Microporous Mesoporous Mater. 246 (2017) 72–80.
[118] W. Qian, F. Sun, Y. Xu, L. Qiu, C. Liu, Energy Environ. Sci. 7 (1) (2014) 379–386.
[119] Z. Ling, Z. Wang, M. Zhang, C. Yu, G. Wang, Y. Dong, S. Liu, Y. Wang, J. Qiu, Adv. Funct. Mater. 26 (1) (2016) 111–119.
[120] X. Tian, H. Ma, Z. Li, S. Yan, L. Ma, F. Yu, G. Wang, X. Guo, Y. Ma, C. Wong, J. Power Sources 359 (2017) 88–96.
[121] J. Wang, Z. Li, S. Yan, X. Yu, Y. Ma, L. Ma, RSC Adv. 9 (2019) 14797–14808.
[122] R. Saidur, E.A. Abdelaziz, A. Demirbas, M.S. Hossain, S. Mekhilef, Renew. Sustain. Energy Rev. 15 (5) (2011) 2262–2289.
[123] J. Xie, C.Y. Hse, C.F. De Hoop, T. Hu, J. Qi, T.F. Shupe, Carbohydr. Polym. 151 (2016) 725–734.
[124] Y. Zhang, S. Liu, X. Zheng, X. Wang, Y. Xu, H. Tang, F. Kang, Q. Yang, J. Luo, Adv. Funct. Mater. 27 (3) (2017), 1604687.
[125] S. Liu, Y. Zhao, B. Zhang, H. Xia, J. Zhou, W. Xie, H. Li, J. Power Sources 381 (2018) 116–126.
[126] S. Lu, M. Jin, Y. Zhang, Y. Niu, J. Gao, C. Li, Adv. Energy Mater. 8 (11) (2018), 1702545.
[127] C. Zhao, Y. Huang, C. Zhao, X. Shao, Z. Zhu, Electrochim. Acta 291 (2018) 287–296.
[128] B. Liu, Y. Liu, H. Chen, M. Yang, H. Li, J. Power Sources 341 (2017) 309–317.
[129] X. Yan, Y. Jia, L. Zhuang, L. Zhang, K. Wang, X. Yao, ChemElectroChem 5 (14) (2018) 1874–1879.
[130] S. Dong, X. He, H. Zhang, X. Xie, M. Yu, C. Yu, N. Xiao, J. Qiu, J. Mater. Chem. 6 (33) (2018) 15954–15960.
[131] B. Liu, X. Zhou, H. Chen, Y. Liu, H. Li, Electrochim. Acta 208 (2016) 55–63.
[132] M. Genovese, K. Lian, J. Mater. Chem. 5 (8) (2017) 3939–3947.
[133] D. Yang, H. Jing, Z. Wang, J. Li, M. Hu, R. Lv, R. Zhang, D. Chen, J. Colloid Interface Sci. 528 (2018) 208–224.
[134] B. Hu, K. Wang, L. Wu, S.H. Yu, M. Antonietti, M.M. Titirici, Adv. Mater. 22 (7) (2010) 813–828.
[135] X. Wu, L. Jiang, C. Long, Z. Fan, Nano Energy 13 (2015) 527–536.
[136] H. Chen, F. Yu, G. Wang, L. Chen, B. Dai, S. Peng, ACS Omega 3 (4) (2018) 4724–4732.
[137] X. Lin, Q. Lü, Q. Li, M. Wu, R. Liu, ACS Omega 3 (10) (2018) 13283–13289.

[138] Y. Zhang, L. Liu, P. Zhang, J. Wang, M. Xu, Q. Deng, Chem. Eng. J. 355 (2019) 309–319.
[139] M. Karnan, K. Subramani, N. Sudhan, N. Ilayaraja, M. Sathish, ACS Appl. Mater. Interfaces 8 (51) (2016) 35191–35202.
[140] C. Wang, Y. Xiong, H. Wang, C. Jin, Q. Sun, J. Mater. Chem. 5 (30) (2017) 15759–15770.
[141] O. Norouzi, S. Jafarian, F. Safari, A. Tavasoli, B. Nejati, Bioresour. Technol. 219 (2016) 643–651.
[142] Y. Huang, Y. Liu, G. Zhao, J.Y. Chen, J. Mater. Sci. 52 (2017) 478–488.
[143] M. Zhou, J. Gomez, B. Li, Y. Jiang, S. Deng, Applied. Mater. Today 7 (2017) 47–54.
[144] C. Wang, D. Wu, H. Wang, Z. Gao, F. Xu, K. Jiang, J. Power Sources 363 (2017) 375–383.
[145] Y. Gong, D. Li, C. Luo, Q. Fu, C. Pan, Green Chem. 19 (17) (2017) 4132–4140.
[146] M. Zhang, Y. Li, H. Si, B. Wang, T. Song, Int. J. Electrochem. Sci. 12 (2017) 7844–7852.
[147] G. Ma, W. Tang, K. Sun, Z. Zhang, E. Feng, Z. Lei, Nano 12 (8) (2017), 1750103.
[148] A.K. Mondal, K. Kretschmer, Y. Zhao, H. Liu, C. Wang, B. Sun, G. Wang, Chemistry 23 (15) (2017) 3683–3690.
[149] J. Cui, Y. Xi, S. Chen, D. Li, X. She, J. Sun, W. Han, D. Yang, S. Guo, Adv. Funct. Mater. 26 (46) (2016) 8487–8495.
[150] R. Thangavel, K. Kaliyappan, H.V. Ramasamy, X. Sun, Y.S. Lee, ChemSusChem 10 (13) (2017) 2805–2815.
[151] D. Yan, C. Yu, X. Zhang, W. Qin, T. Lu, B. Hu, H. Li, L. Pan, Electrochim. Acta 191 (2016) 385–391.
[152] R. Gaddam, D. Yang, R. Narayan, K. Raju, N. Kumar, X. Zhao, Nano Energy 26 (2016) 346–352.
[153] T. Rufford, D. Hulicova-Jurcakova, K. Khosla, Z. Zhu, G. Lu, J. Power Sources 195 (2010) 912–918.
[154] S. Gao, Y. Chen, Y. Fan, X. Wei, C. Hu, H. Luo, L. Qu, J. Mater. Chem. 2 (10) (2014) 3317.
[155] L. Tao, Y. Huang, Y. Zheng, X. Yang, C. Liu, M. Di, S. Larpkiattaworn, M. Nimlos, Z. Zheng, J. Taiwan. Inst. Chem. Eng. 95 (2019) 217–226.
[156] C. Wang, J. Huang, H. Qi, L. Cao, Z. Xu, Y. Cheng, X. Zhao, J. Li, J. Power Sources 358 (2017) 85–92.
[157] L. Wang, G. Mu, C. Tian, L. Sun, W. Zhou, P. Yu, J. Yin, H. Fu, ChemSusChem 6 (5) (2013) 880–889.
[158] X. Zheng, W. Lv, Y. Tao, J. Shao, C. Zhang, D. Liu, J. Luo, D. Wang, Q. Yang, Chem. Mater. 26 (23) (2014) 6896–6903.
[159] P. Hao, Z. Zhao, J. Tian, H. Li, Y. Sang, G. Yu, H. Cai, H. Liu, C. Wong, A. Umar, Nanoscale 6 (20) (2014) 12120–12129.
[160] J. Huang, B.G. Sumpter, V. Meunier, Chemistry 14 (22) (2008) 6614–6626.
[161] E. Frackowiak, Phys. Chem. Chem. Phys. 9 (15) (2007) 1774–1785.
[162] D. Wang, F. Li, M. Liu, G. Lu, H. Cheng, J. Phys. Chem. C 112 (2008) 9950–9955.
[163] X. Xu, J. Zhou, D.H. Nagaraju, L. Jiang, Val R. Marinov, G. Lubineau, Husam N. Alshareef, M. Oh, Adv. Funct. Mater. 25 (21) (2015) 3193–3202.
[164] J. Wang, S. Kaskel, J. Mater. Chem. 22 (45) (2012) 23710.
[165] L.L. Zhang, H.H. Li, Y.H. Shi, C.Y. Fan, X.L. Wu, H.F. Wang, H.Z. Sun, J.P. Zhang, ACS Appl. Mater. Interfaces 8 (6) (2016) 4233–4241.
[166] J. Hao, C. Cao, F. Idrees, X. Ma, ACS Nano 9 (3) (2015) 2556–2564.
[167] D. Zhou, W. Li, X. Dong, Y. Wang, C. Wang, Y. Xia, J. Mater. Chem. 1 (29) (2013) 8488.
[168] H. Lu, L. Zhuang, R. Gaddam, X. Sun, C. Xiao, T. Duignan, Z. Zhu, X. Zhao, J. Mater. Chem. 7 (39) (2019) 22579–22587.
[169] M. Liu, K. Zhang, M. Si, H. Wang, L. Chai, Y. Shi, Carbon 153 (2019) 707–716.
[170] C. Huang, T. Sun, D. Hulicova-Jurcakova, ChemSusChem 6 (12) (2013) 2330–2339.
[171] G. Xu, J. Han, B. Ding, P. Nie, J. Pan, H. Dou, H. Li, X. Zhang, Green Chem. 17 (3) (2015) 1668–1674.
[172] J. Jimenez, M. Skalic, G. Martinez-Rosell, G. De Fabritiis, J. Chem. Inf. Model. 58 (2) (2018) 287–296.
[173] D.P. Tabor, L.M. Roch, S.K. Saikin, C. Kreisbeck, D. Sheberla, J.H. Montoya, S. Dwaraknath, M. Aykol, C. Ortiz, H. Tribukait, C. Amador-Bedolla, C.J. Brabec, B. Maruyama, K.A. Persson, A. Aspuru-Guzik, Nat. Reviews Mater. 3 (5) (2018) 5–20.
[174] J.D. Perea, S. Langner, M. Salvador, B. Sanchez-Lengeling, N. Li, C. Zhang, G. Jarvas, J. Kontos, A. Dallos, A. Aspuru-Guzik, C.J. Brabec, J. Phys. Chem. C 121 (33) (2017) 18153–18161.
[175] H. Su, C. Lian, J. Liu, H. Liu, Chem. Eng. Sci. 202 (2019) 186–193.
[176] M. Zhou, A. Gallegos, K. Liu, S. Dai, J. Wu, Carbon 157 (2020) 147–152.
[177] H. Chaoui, C.C. Ibe-Ekeocha, H. Gualous, Elec. Power Syst. Res. 146 (2017) 189–197.
[178] J. Mozaryn, A. Chmielewski, IFAC PapersOnLine 51 (2018) 23–30.
[179] H. Farsi, F. Gobal, Comput. Mater. Sci. 39 (3) (2007) 678–683.
[180] T.D. Dongale, P.R. Jadhav, G.J. Navathe, J.H. Kim, M.M. Karanjkar, P.S. Patil, Mater. Sci. Semicond. Process. 36 (2015) 43–48.
[181] T. Weigert, Q. Tian, K. Lian, J. Power Sources 196 (2011) 4061–4066.
[182] S. Zhu, J. Li, L. Ma, C. He, E. Liu, F. He, C. Shi, N. Zhao, Mater. Lett. 233 (2018) 294–297.
[183] J. Wang, F. Li, F. Zhu, O. Schmidt, Small Methods (2018) 1800367.
[184] S. Herou, P. Schlee, A.B. Jorge, M. Titirici, Curr. Opin. Green Sustain. Chem. 9 (2018) 18–24.